ChemComm

FEATURE ARTICLE

View Article Online
View Journal | View Issue

Published on 22 June 2016. Downloaded by Library for Natural Sciences of the RAS on 8/27/2018 10:11:04 AM.

Cite this: *Chem. Commun.*, 2016, **52**, 10322

Molecular recognition and activation by polyaza macrocyclic compounds based on host–guest interactions

Di-Chang Zhong[ab] and Tong-Bu Lu*[ac]

Received 2nd May 2016,
Accepted 22nd June 2016

DOI: 10.1039/c6cc03660k

www.rsc.org/chemcomm

The design and syntheses of supramolecular hosts for the recognition and activation of molecules and anions are one of the most active research fields in supramolecular chemistry, in which polyaza macrocyclic ligands and their complexes have drawn particular attention due to their strong host–guest interactions. This review mainly focuses on the recent progress in the recognition of molecules and anions by polyaza macrocyclic compounds including polyaza macrocycles, polyaza macrobicycles and polyaza macrotricycles, as well as the activation of molecules by polyaza macrocyclic ligands and their metal complexes.

Introduction

Host–guest chemistry, describing the complexes composed of two or more molecules/ions held together by forces other than covalent bonds, is an important part of the research subjects in supramolecular chemistry. In host–guest interaction, recognition between the acceptor and the substrate is an initial and indispensable process. Elucidation of the recognition principles should date back to the late nineteenth century. In 1894, Hermann Emil Fischer, a farsighted chemist, put forward his brilliant "lock-and-key" idea and suggested that enzymes and substrates can be compared to "lock and key" for understanding their selectivity.[1] Then it was Paul Ehrlich who recognized that molecules do not act if they do not bind.[2] Finally, Alfred Werner introduced the idea of coordination to illustrate the binding/fixation interaction affinity between partners.[3] Based on these great basic concepts, molecular recognition science

[a] *Institute of New Energy Materials & Low Carbon Technology, School of Material Science & Engineering, Tianjin University of Technology, Tianjin 300384, China. E-mail: lutongbu@mail.sysu.edu.cn*
[b] *Key Laboratory of Jiangxi University for Functional Material Chemistry, College of Chemistry & Chemical Engineering, Gannan Normal University, Ganzhou 341000, P. R. China*
[c] *MOE Key Laboratory of Bioinorganic and Synthetic Chemistry, School of Chemistry and Chemical Engineering, Sun Yat-Sen University, Guangzhou 510275, China*



Di-Chang Zhong

Di-Chang Zhong (1981) obtained his BS in 2003 from Gannan Normal University, Ganzhou, China, and MS in 2006 from Guangxi Normal University under the supervision of Prof. Z. F. Chen, and PhD in 2011 from Sun Yat-Sen University under the supervision of Prof. T. B. Lu. Then he worked as a JSPS postdoctoral fellow at AIST, Japan. In 2016, he joined the faculty at the Tianjin University of Technology as a professor. His interests focus on porous crystalline materials used for storage of clean energy.



Tong-Bu Lu

Tong-Bu Lu (1964) obtained his BS in 1988 and PhD in 1993 under the supervision of Prof. Min-Yu Tan from Lanzhou University. After two years of postdoctoral fellowship at Sun Yat-Sen University, he joined the faculty at the same University, and became a professor in 2000. In 1998 and 2002, he worked as a postdoctoral fellow in F. A. Cotton's group at Texas A&M University. He moved to the Tianjing University of Technology in 2016. His research interest is in supramolecular chemistry, including macrocyclic chemistry, MOFs and pharmaceutical polymorphs and cocrystals. Currently he focuses on the activation of water and CO_2 using polyaza macrocyclic metal complexes and related compounds as catalysts for the production of clean and renewable energy.

This journal is © The Royal Society of Chemistry 2016

Published on 22 June 2016. Downloaded by Library for Natural Sciences of the RAS on 8/27/2018 10:11:04 AM.

has rapidly developed and the host–guest chemistry has become the core of supramolecular chemistry.

Recognition of guest molecules by a host needs driving forces, which are usually non-covalent bonding interactions.[4] There are four commonly mentioned types of non-covalent interactions, including electrostatic interactions, hydrogen bonds, van der Waals forces, and hydrophobic interactions. Besides driving forces, complementarity between host and guest molecules is the other important factor that affects recognition.[5] The success of molecular recognition lies in establishing a precise complementarity between the associating partners. Complementarity should take two forms, one is that the shape and size of the receptor cavity must complement the form of the substrate, and the other is that the binding site surrounding the receptor must complement the preference of the substrate.[6] The more binding regions (contact area) present, the stronger and more selective will be the recognition. On the basis of the driving force and complementarity, the host and guest naturally recognize and combine together to form a receptor–substrate complex.

Molecular recognition plays a critical role in biological processes. It may be said that without molecular recognition, there would be no life in this world, as vital biochemical processes including enzyme action, molecular transport, genetic information, and protein assembly all involve molecular recognition.[7] However, a detailed understanding of these complicated biochemical processes is still a challenge. Host–guest complexes in supramolecular chemistry are useful models for understanding the process of molecular recognition in biological systems. Such complexes have a small size relative to much larger biomacromolecule–substrate complexes, and thus converged results can be obtained rapidly, which offers the opportunity to make clear some fundamental aspects of the binding thermodynamics between the biomacromolecule and the substrate. This also provides constructive guidance for drug design.[8] Therefore, it is very meaningful to investigate molecular recognition from the perspective of chemistry.

Molecular activation follows molecular recognition and subsequent host–guest binding. Exactly speaking, the activation of molecules is the result of the recognition and interaction of molecules. Molecular activation exists widely in chemical and biological systems, such as enzymes perform their biological functions to catalyze the substrate to product conversion, where the substrate will firstly be activated.[9] During the host–guest interaction, the host binds to the functional group of the guest molecule and thus the adjacent groups/bonds to the functional group will be weakened. In the activated state, the molecules usually exhibit an increased propensity to undergo a specified chemical reaction.

In the host–guest chemistry, macrocyclic ligands, including crown ethers,[10] calixarenes,[11] cucurbiturils,[12] pillararenes,[13] and so on, are a class of typical examples of host molecules. During the past several decades, there is continuous interest in the design and synthesis of new macrocyclic receptors for molecular recognition and activation.[14] Polyaza macrocyclic ligands have drawn particular attention.[15] The reasons may be ascribed to two aspects. One is that the polyaza macrocyclic compounds containing multiple nitrogen atoms, no matter in aqueous or non-aqueous solution; the basicity of amines and the pK_a values of these polyaza macrocyclic ligands can be adjusted by diverse protonation. These resulting ligands with different degrees of protonation exhibit different recognition abilities to molecules or anions. In addition, host concentrations, counter-anions and temperature will also have significant impact on the protonation–deprotonation equilibrium. Thus the recognition abilities of these polyaza macrocyclic hosts to molecules or anion guests can be precisely adjusted by changing the above factors. The other is that the polyaza macrocyclic compounds are readily synthesized and possess high stability, as well as easily form complexes with metal ions. The resulting complexes also show recognition and activation of molecules or anions.

In this review, we mainly focus on the recent progress in the recognition of molecules and anions by polyaza macrocyclic compounds including polyaza macrocycles, macrobicycles and macrotricycles, as well as the activation of molecules and anions by polyaza macrocyclic ligands and their metal complexes.

1. Recognition of polyaza macrocycles

Despite containing multiple binding sites, the interactions of polyaza macrocycles (monocycles) with substrate molecules are less effective, due to the lack of space confinements in substrate molecules. In early macrocyclic chemistry studies, a number of polyaza macrocycles containing functional groups, such as ureas, thioureas, amides, thioamides, pyrroles and so on, have been designed and synthesized.[16] These ligands possess different membered rings and thus show different recognition capacities. Mani's group systematically investigated the recognition of pyrrole-based polyaza macrocycles. They firstly synthesized azatripyrrolic ($\mathbf{L^1}$) and azatetrapyrrolic macrocycles ($\mathbf{L^2}$) in a single step by the Mannich reaction of pyrrole in the presence of primary amine hydrochloride (Fig. 1). ^{1}H NMR titrations have revealed that both macrocycles show large binding constants for the halide anion and exhibit different binding stoichiometries.[17] Then they designed and synthesized macrocycles $\mathbf{L^3}$ (Fig. 2a), which contain both hydrogen bond donors (NH) and acceptors (tertiary amine groups) in the cleft (Fig. 2b). Upon binding to the SO_4^{2-} anion, a great

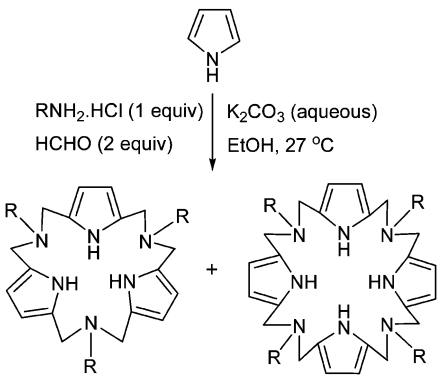


Fig. 1 Syntheses of (left) azatripyrrolic macrocycle ($\mathbf{L^1}$) and (right) azatetrapyrrolic macrocycle ($\mathbf{L^2}$).

Published on 22 June 2016. Downloaded by Library for Natural Sciences of the RAS on 8/27/2018 10:11:04 AM.

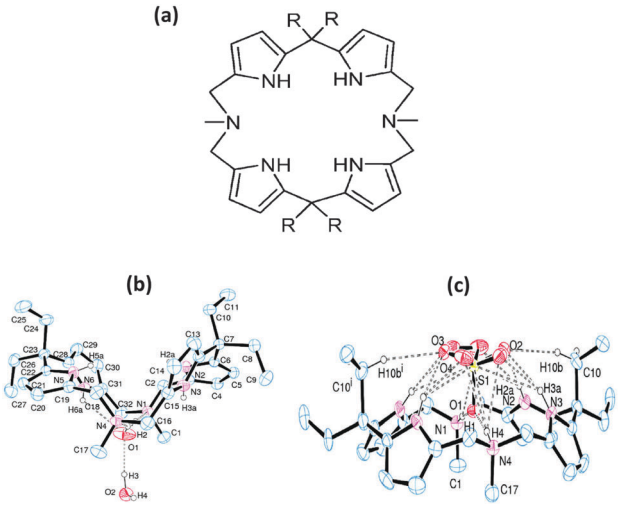


Fig. 2 (a) Chemical structure of $\mathbf{L^3}$. Crystal structures of (b) $L^3{\cdot}2H_2O$ and (c) protonated $\mathbf{L^3}$ combined with the SO_4^{2-} anion.

conformational change of the protonated $\mathbf{L^3}$ occurs (Fig. 2c). Additionally, the competition experiments demonstrated that only the sulfate complex can be crystallized in more than 85% yield, suggesting geometric and electrostatic complementarities between protonated $\mathbf{L^3}$ and the SO_4^{2-} anion.[18] By Schiff base condensation reactions, Mani and co-workers further prepared a series of large size polyaza macrocycles containing *N*,*N*-di(pyrrolylmethyl)-*N*-methylamine moieties and different linkers ($\mathbf{L^4}$ and $\mathbf{L^5}$, Fig. 3). The anion binding investigations of $\mathbf{L^4}$ and $\mathbf{L^5}$ by NMR titration have shown that although they have similar pyrrolic and amine NH groups, their binding properties are different, in which $\mathbf{L^4}$ with ethylene as a linker binds anions in a 1 : 1 fashion, while $\mathbf{L^5}$ with phenylene as a linker prefers to bind anions in a sequential 1 : 2 fashion. These results can be attributed to the different conformational flexibility of the linkers in the receptors.[19]

The imidazolium unit is also an ideal motif used to construct macrocyclic ligands for anion recognition due to its inherently cationic and hydrogen-bond donating characteristics. You and co-workers designed and synthesized a rigid tetrakisimidazolium

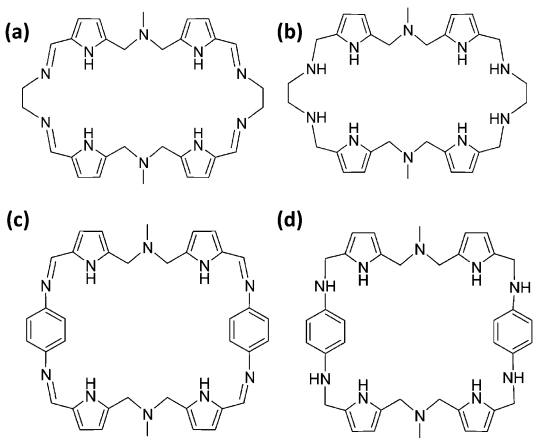


Fig. 3 Chemical structure of (a) $\mathbf{L^4}$ and (b) its reduced product, as well as (c) $\mathbf{L^5}$ and (d) its reduced product.

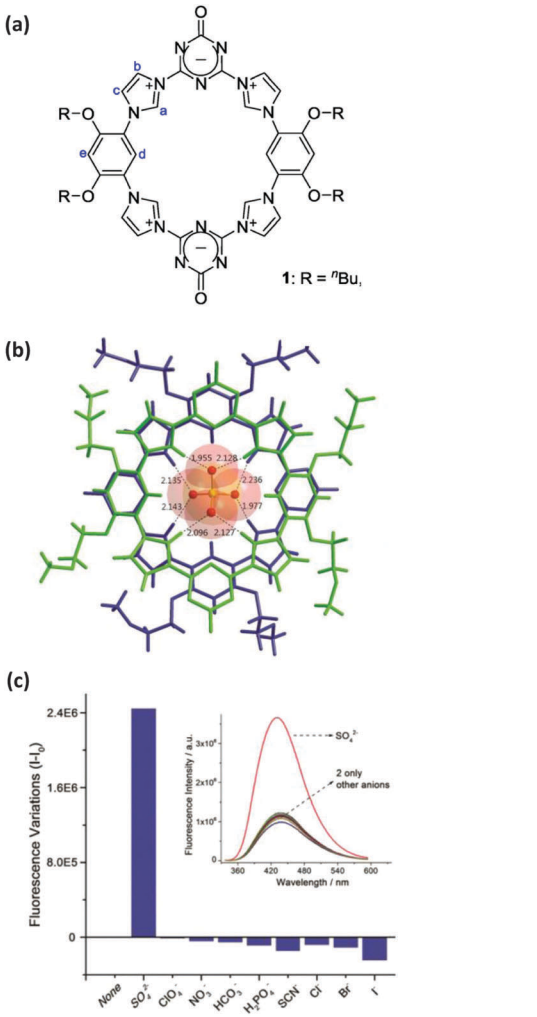


Fig. 4 (a) Chemical structure of $\mathbf{L^6}$. (b) Crystal structure of $\mathbf{L^6}$ incorporated with SO_4^{2-}. (c) Fluorescence variations and fluorescence spectra (inset) of $\mathbf{L^6}$ (10 μM) upon the addition of 20 equiv. of anions in 10 mM HEPES buffer at pH 7.0, excited at 304 nm.

based polyaza macrocycle $\mathbf{L^6}$ (Fig. 4a). They found that $\mathbf{L^6}$ can selectively bind a hydrophilic sulfate anion over other anions by forming a 2 : 1 complex (Fig. 4b), with a large association constant of 8.6×10^9 M^{-2} and a perceptible fluorescence enhancement (Fig. 4c). This highly selective binding, investigated by X-ray diffraction analysis, is attributed to: (1) the electrostatic interactions and the eight strong hydrogen bonds between the cationic imidazoliums and anionic sulfate; (2) the pseudo "geometric fit" cavity suitable for sulfate; (3) the π–π stacking and charge-assisted hydrogen bonds between two host macrocycles; and (4) the flexible peripheral chains serving as the shield around the seam of the complex to protect the sulfate from being attacked by the highly competitive solvents. $\mathbf{L^6}$ could be used as a fluorescence detector for the sulfate anion in the aqueous environment.[20]

Pyridazine has also been introduced into polyaza macrocyclic ligands for molecular recognition. The Wang group has synthesized water-soluble S6-corona[3]arene[3]pyridazines ($\mathbf{L^7}$, Fig. 5a) by an efficient and scalable synthetic pathway.[21] The synthesis

 This journal is © The Royal Society of Chemistry 2016

Published on 22 June 2016. Downloaded by Library for Natural Sciences of the RAS on 8/27/2018 10:11:04 AM.

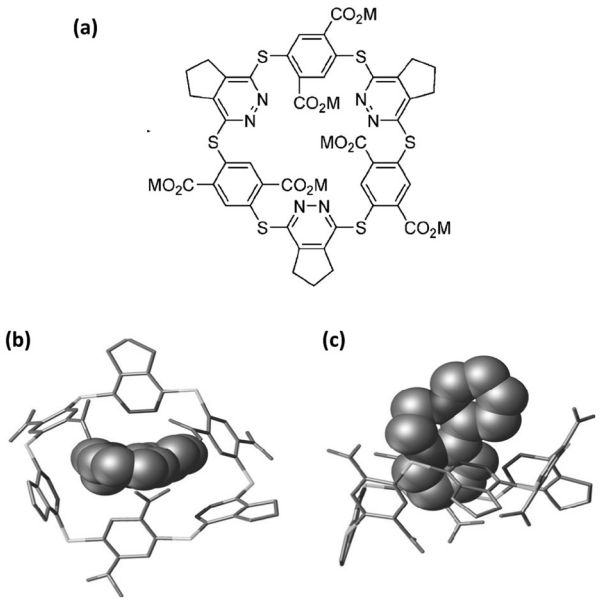


Fig. 5 (a) Chemical structure of $\mathbf{L^7}$, (b) and (c) crystal structures of $\mathbf{L^7}$ with a dicationic guest.

comprises a one-pot nucleophilic aromatic substitution reaction between diesters of 2,5-dimercaptoterephthalate and 3,6-dichlorotetrazine, followed by the inverse electron-demand Diels–Alder reaction of the tetrazine moieties with enamine and exhaustive saponification of esters. The resulting $\mathbf{L^7}$ adopts a 1,3,5-alternate conformation in the crystalline state and is able to selectively form stable 1 : 1 complexes with dicationic guest species in water, with association constants ranging from $(1.10 \pm 0.06) \times 10^3$ M^{-1} to $(1.18 \pm 0.06) \times 10^5$ M^{-1} (Fig. 5b and c).

Upon complexation with metal ions, the resulting complexes are expected to be more rigid than the corresponding ligands, and may also show recognition functions. Mendy *et al.* synthesized a polyaza macrocycle ($\mathbf{L^8}$, Fig. 6a) and its dinuclear Cu(II) complex of $[Cu_2L^8Br_3(H_2O)]Br$. X-ray crystallography revealed that $\mathbf{L^8}$ is folded to form a bowl-shaped cavity (Fig. 6b), which exhibits a strong affinity and selectivity for iodide (Fig. 6c).[22]

We have developed an anthracene-based polyaza macrocycle of $\mathbf{L^9}$. Upon complexation with Zn(II), the resulting $[Zn_2L^9](ClO_4)_4$ (Fig. 7) is found to be an excellent fluorescent chemosensor, which can effectively and selectively recognize adenosine polyphosphates (ATP and ADP) over other structurally similar nucleoside polyphosphates in aqueous solution at a physiological pH of 7.40, with a large fluorescence enhancement (F_{max}/F_0 = 70 and 80 for ATP and ADP, respectively) and strong binding affinity ($K > 10^{11}$ M^{-1}).[23] This high selectivity can be attributed to the multiple host–guest interactions. That is, the two Zn(II) ions in $\mathbf{L^9}$ can catch two ATP/ADP anions through coordination interactions between Zn(II) and the polyphosphate groups, and the two anthracene moieties in $\mathbf{L^9}$ can interact with adenine groups of ATP/ADP anions through stacking interactions; these multiple recognition interactions between $[Zn_2L^9]^{4+}$ and ATP/ADP enhance the affinity and selectivity of $[Zn_2L^9]^{4+}$ toward ATP/ADP.

A chiral polyaza macrocyclic complex can be used as a receptor to recognize a chiral substrate. $\mathbf{L^{10}}$ (Fig. 8a and b) is a typical tetraaza

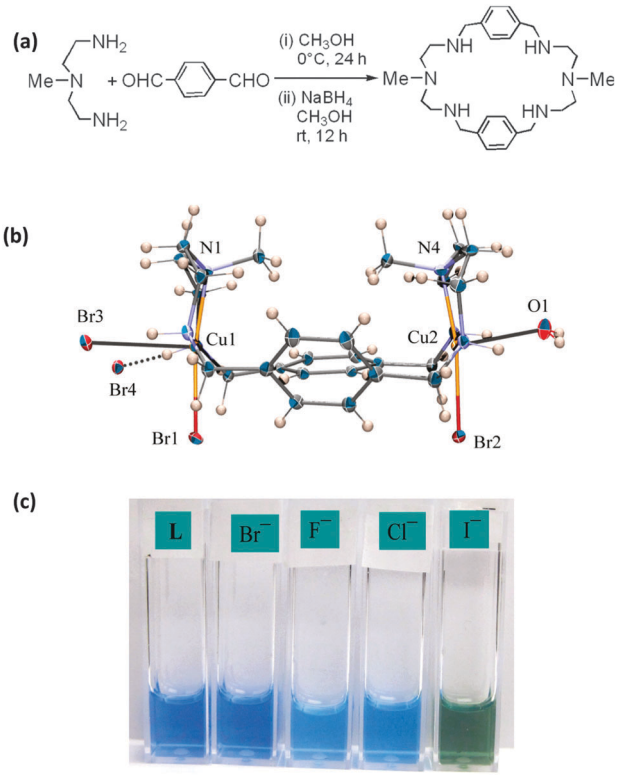


Fig. 6 (a) The synthesis of $\mathbf{L^8}$ and (b) crystal structure of $[Cu_2L^8Br_3(H_2O)]Br$. (c) Color changes of $[Cu_2L^8Br_3(H_2O)]Br$ upon addition of halides.

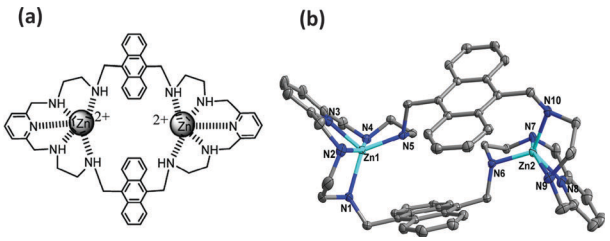


Fig. 7 (a) Chemical and (b) crystal structure of $[Zn_2L^9]^{4+}$.

macrocyclic ligand. Its nickel(II) complexes have two diastereomers of *meso* and *rac* (racemic) forms.[24] $[Ni(meso\text{-}L^{10})]^{2+}$, with the two asymmetric carbon atoms adopting opposite (*R* and *S*) configurations in $\mathbf{L^{10}}$, has shown electrocatalytic activities for water reduction to produce H_2 and water oxidation to produce O_2, found by the Eisenberg group over three decades ago[25] and our group very recently.[26] $[Ni(rac\text{-}L^{10})]^{2+}$, with two asymmetric carbon atoms adopting the same (*RR* or *SS*) configuration in $\mathbf{L^{10}}$, exhibited highly selective recognition to chiral amino acid molecules. For instance, the *RR* and *SS* enantiomers in $[Ni(\alpha\text{-}rac\text{-}L^{10})]^{2+}$ show high recognition capacity to D and L-Phe^- in racemic phenylalanine (Phe), to yield $[Ni(SS\text{-}L^{10})(L\text{-}Phe)]^+$ and $[Ni(RR\text{-}L^{10})(D\text{-}Phe)]^+$ with a 1D right-handed homochiral helical chain and a 1D left-handed homochiral helical chain, respectively (Fig. 8c–f).[27] Obviously, the spontaneous resolution occurs during the reaction, as each crystal crystallizes into one enantiopure. Additionally, upon mixing $[Ni(SS\text{-}L^{10})(D\text{-}Phe)](ClO_4)$ and $[Ni(RR\text{-}L^{10})(L\text{-}Phe)](ClO_4)$, the *SS* and *RR* enantiomers preferentially coordinate to L- and D-Phe

Published on 22 June 2016. Downloaded by Library for Natural Sciences of the RAS on 8/27/2018 10:11:04 AM.

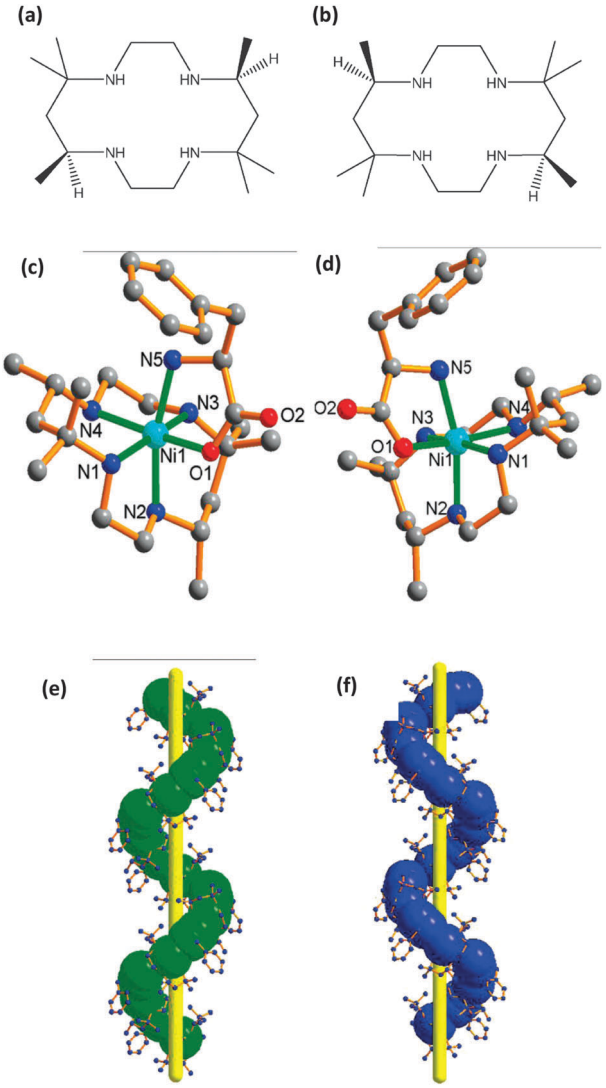


Fig. 8 Chemical structures of (a) *SS*-5,5,7,12,12,14-hexamethyl-1,4,8,11-tetraazacyclotetradecane (*SS*-**L^{10}**) and (b) *R*-5,5,7,12,12,14-hexamethyl-1,4,8,11-tetraazacyclotetradecane (*RR*-**L^{10}**). Crystal structures of (c) [Ni(*SS*-L^{10})-(L-Phe)]$^{+}$ and (d) [Ni(*RR*-L^{10})(D-Phe)]$^{+}$. 1D hydrogen bonded (e) right-handed helical chain and (f) left-handed helical chain.

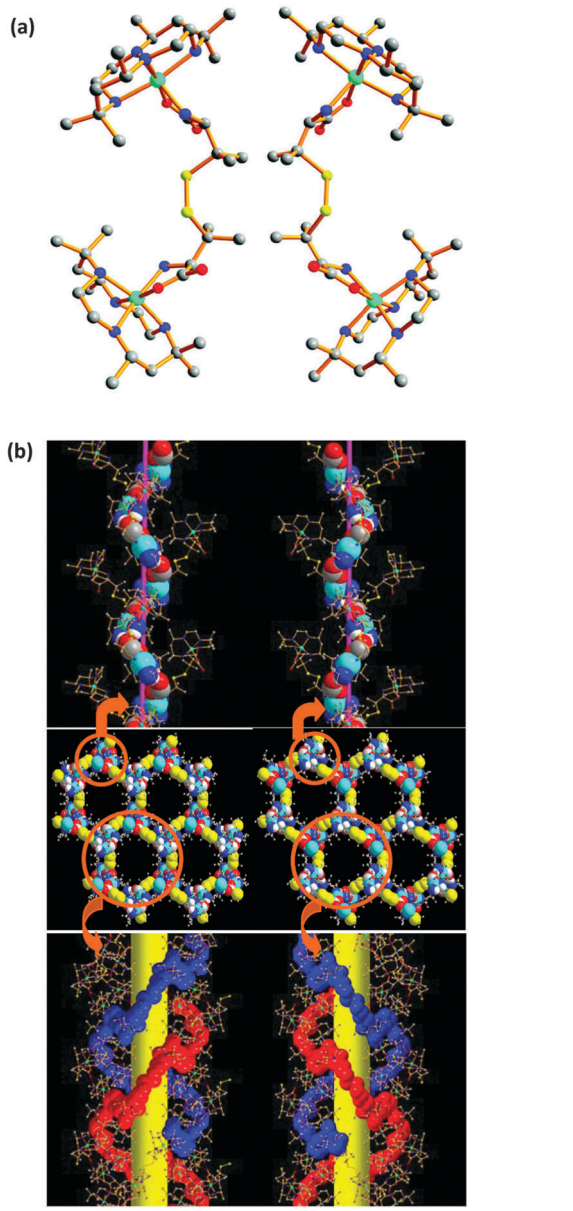


Fig. 9 (a) A pair of enantiomers of {[Ni(*SS*-L^{10})]$_2$(L-pends)}$^{2+}$ and {[Ni(*RR*-L^{10})]$_2$(D-pends)}$^{2+}$. (b) 3D supramolecular frameworks of {[Ni(*SS*-L^{10})]$_2$(L-pends)}$_n^{2n+}$ and {[Ni(*RR*-L^{10})]$_2$(D-pends)}$_n^{2n+}$ possessing 1D chrial pores with opposite right and left-handed helical porous surfaces, respectively.

respectively, to form two stable enantiomers of [Ni(*SS*-L^{10})(L-Phe)]-(ClO$_4$) and [Ni(*RR*-L^{10})(D-Phe)](ClO$_4$), further revealing the high chiral recognition ability by chiral macrocyclic complexes of [Ni(*SS*-L^{10})]$^{2+}$ and [Ni(*RR*-L^{10})]$^{2+}$.[27]

[Ni(α-*rac*-L^{10})](ClO$_4$)$_2$ containing equal amounts of *SS* and *RR* enantiomers also shows chiral recognition to L and D-penicillamine (Pen), respectively. Spontaneous resolution occurs during the reaction of racemic [Ni(α-*rac*-L^{10})](ClO$_4$)$_2$ with racemic penicillamine to get a pair of enantiomers of {[Ni(*SS*-L^{10})]$_2$(L-pends)}$^{2+}$ and {[Ni(*RR*-L^{10})]$_2$(D-pends)}$^{2+}$ (Fig. 9a),[28] in which [Ni(*SS*-L^{10})]$^{2+}$ and [Ni(*RR*-L^{10})]$^{2+}$ recognize L- and D-pends, respectively (pends^{2-} = penicillamine disulfide anion, formed by the oxidation of Pen by atmospheric oxygen). {[Ni(*SS*-L^{10})]$_2$(L-pends)}$^{2+}$ and {[Ni(*RR*-L^{10})]$_2$-(D-pends)}$^{2+}$ are further connected by intermolecular hydrogen bonds to generate a pair of 3D homochiral supramolecular frameworks, possessing 1D tubular pores with opposite right/left-handed helical porous surfaces, respectively (Fig. 9b). Additionally, the *SS* and *RR* enantiomers in [Ni(α-*rac*-L^{10})]$^{2+}$ can also recognize L and D-leucine (Leu) in acetonitrile/water under acidic conditions to give the left-handed helical chains of [Ni(*SS*-L^{10})(L-HLeu)](ClO$_4$)$_2$ and right-handed helical chains of [Ni(*RR*-L^{10})(D-HLeu)](ClO$_4$)$_2$, respectively.[29]

2. Recognition of polyaza macrobicycles (cryptands)

Compared with macrocycles, polyaza macrobicycles (also called cryptands) are relatively rigid. They usually exhibit strong affinities to the substrates due to their specific structures containing

 This journal is © The Royal Society of Chemistry 2016

Published on 22 June 2016. Downloaded by Library for Natural Sciences of the RAS on 8/27/2018 10:11:04 AM.

multi-binding sites. Additionally, cryptands are readily combined with metal ions to form cryptates, which also show recognition to certain substrates.

2.1 Polyaza cryptands

2.1.1 Polyaza cryptands with aliphatic chain spacers. Bistren connected by aliphatic chain spacers are a class of early studied polyaza cryptands as anion receptors. In a pioneering work, Lehn and co-workers investigated the synthesis, binding and crystal structure of a fluoride inclusion complex with a hexaprotonated azacryptand, which later came to be known as the tiny octaaza-cryptand $\mathbf{L^{11}}$ (Fig. 10a).[30] At that time, this tiny cryptand was found to possess high selectivity for fluoride over other halide anions, attributed to the small size of the cryptand cavity. The log K value reaches as high as 10.55 in aqueous solution. A decade later, Bowman-James *et al.* found that encapsulation of F^-/Cl^- into the cavity of $\mathbf{L^{11}}$ is pH-dependent. In the pH range of 5.5–2.5, only fluoride binds strongly, and at pH $\leq$ 2.5, a dramatic increase in the affinity for chloride occurs. They showed the crystal structure of a hexaprotonated chloride complex, in which Cl^- anions are encapsulated inside the cryptand cavity.[31] Ghosh *et al.* further provided structural evidence on halide selectivity inside this tiny cage. They firstly obtained a bromide complex of hexaprotonated $\mathbf{L^{11}}$, which showed no guest encapsulation inside the tiny cage (Fig. 11a). Then they used $[H_6L^{11}]Br_6$ as a receptor to capsulate the mixed anions of F^-/Br^- and Cl^-/Br^-, generating two complexes $[H_6L^{11}F]Br_5$ (Fig. 11b) and $[H_6L^{11}Cl]Br_5$ (Fig. 11c), respectively, in which F^- and Cl^- anions were encapsulated inside the cavity of $\mathbf{L^{11}}$, and the Br^- anions located outside the cavity as counteranions.[32]

Cryptand $\mathbf{L^{12}}$ (Fig. 10b) is also an early studied receptor by Lehn and co-workers, which can be considered as a derivative of $\mathbf{L^{11}}$ with a longer aliphatic chain. $\mathbf{L^{12}}$ has been found to be capable of encapsulating halide anions, with a definite trend that the binding affinities decrease with increasing halide size. This is evidenced by the binding constants of log K = 4.1, 3.0, 2.6 and 2.15 of $[H_6\mathbf{L^{12}}]^{6+}$ for fluoride, chloride, bromide and iodide, respectively. The F^- anion sits at one side of the cavity, forming H-bonds with only four of the protonated cryptand amines, and the Cl^- and Br^- anions locate at the center of the cavity. The distance between the bridgehead N atoms is 7.66, 7.40 and 7.50 Å for fluoride, chloride and bromide complexes, respectively.[33]

2.1.2 Polyaza cryptands with aromatic or heterocyclic spacers. Using the aromatic or heterocyclic spacers instead of aliphatic chain spacers, the windows and cavities of the formed cryptands decrease. $\mathbf{L^{13}}$ is a typical polyaza cryptand with aromatic rings as spacers (Fig. 12a). The hexaprotonated azacryptand $[H_6L^{13}]^{6+}$ can easily encapsulate F^-, Cl^- and Br^- inside its cavity to generate cascade complexes under different conditions, while for I^- with a larger diameter, heating is a necessary step for incorporation of I^- into its cavity.[34] This result clearly demonstrates that the cavity of $\mathbf{L^{13}}$ is large enough to accommodate all halide anions within its cavity. However, the halide anion needs firstly to pass through the windows of the crytands, which are flexible and responsive to the external conditions.

$[H_6L^{13}]^{6+}$ also shows the ability to recognize tetrahedral anions.[35] At room temperature, the cavity of $[H_6L^{13}]^{6+}$ can encapsulate ClO_4^- at pH = 2 to form a cascade complex of $[H_6L^{13}(ClO_4)]^{5+}$ (Fig. 13a), while it cannot encapsulate larger $H_2PO_4^-$ within its cavity due to the window limitation, and the reactions of $\mathbf{L^{13}}$ with H_3PO_4 at pH = 1 gives $[H_8L^{13}(H_2O)_3](H_2PO_4)_8$ (Fig. 13b). At higher temperature, however, the window of the protonated $\mathbf{L^{13}}$ can be enlarged, in this case, $H_2PO_4^-$ successfully passes through the window to enter the cavity of $[H_8L^{13}]^{8+}$ to generate a cascade complex of $[H_8L^{13}(H_2PO_4)]^{7+}$ (Fig. 13c). These observations indicate that the encapsulation of tetrahedral anions by the protonated cryptand $\mathbf{L^{13}}$ is both size and temperature dependent. SO_4^{2-} can also be encapsulated inside the cavity of protonated cryptands of $[H_8\mathbf{L^{14}}]^{8+}$ (Fig. 12b) to generate a cascade complex of $[H_8L^{14}(SO_4)](SO_4)_2(HSO_4)_2$.[36]

Besides the above-mentioned tetrahedral anions, $[H_6L^{13}]^{6+}$ can also encapsulate $^{99}TcO_4^-$. Amendola and co-workers have found that $[H_6L^{13}]^{6+}$ shows high affinity to $^{99}TcO_4^-$ in water. The affinity constant is over 5.5 logarithmic units, about two and three orders of magnitude higher than those of perchlorate and nitrate, respectively. Crystal structure investigations reveal that the outstanding affinity for TcO_4^- is due to the complementarity

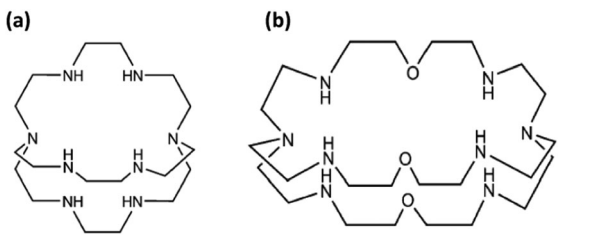


Fig. 10 Aliphatic polyaza macrocyclic ligands of (a) 1,4,7,10,13,16,21,24-octaazabicyclo[8.8.8]hexacosane ($\mathbf{L^{11}}$) and (b) 7,19,30-trioxa-1,4,10,13,16,-22,27,33-octaazabicyclo[11.11.11]pentatriacontane ($\mathbf{L^{12}}$).

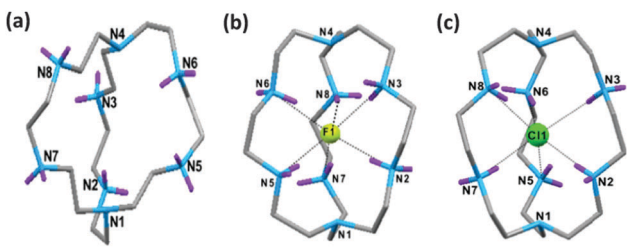


Fig. 11 Structures of (a) $[H_6L^{11}]Br_6$, (b) $[H_6L^{11}F]Br_5$ and (c) $[H_6L^{11}Cl]Br_5$.

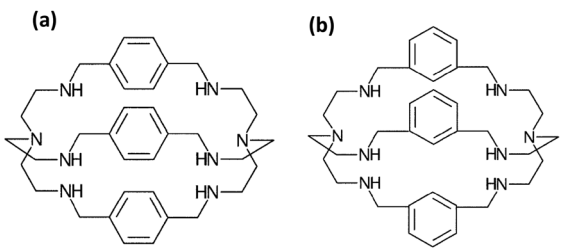


Fig. 12 Chemical structures of (a) 1,4,11,14,17,24,29,36-octa-azapentacyclo-[12.12.12.2^{6,9}.2^{19,22}.2^{31,34}]-tetratetraconta-6(43), 7,9(44),19(41),20,22(42),31(39),-32,34(40)-nonaene ($\mathbf{L^{13}}$) and (b) $\mathbf{L^{14}}$.

Published on 22 June 2016. Downloaded by Library for Natural Sciences of the RAS on 8/27/2018 10:11:04 AM.

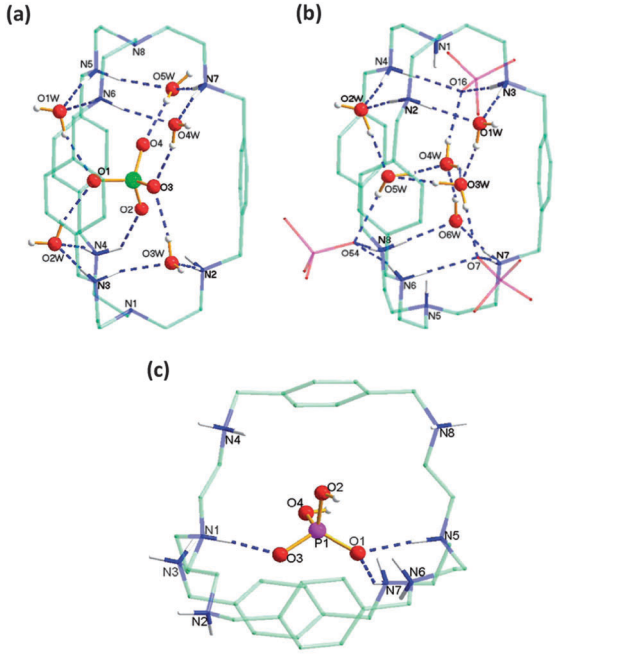


Fig. 13 Crystal structures of (a) $[H_6L^{13}(ClO_4)]^{5+}$, (b) $[H_8L^{13}(H_2O)_3](H_2PO_4)_8$, (c) $[H_8L^{13}(H_2PO_4)]^{7+}$.

between the receptor's cavity and the TcO_4^- anion (Fig. 14a).[37] Then they have improved the molecular system by introducing a fluorescent signaling unit in the receptor's skeleton, that is, using $\mathbf{L^{15}}$ to encapsulate TcO_4^- (Fig. 14b). In water, at pH = 2, upon addition of TcO_4^-, the fluorescence of hexaprotonated $\mathbf{L^{15}}$ is switched off, following the formation of a stable 1 : 1 inclusion complex (Fig. 14c).[38] This sensitive response makes hexaprotonated $\mathbf{L^{15}}$ an excellent fluorescent chemosensor for $^{99}TcO_4^-$ in water (Fig. 14d).

In addition to anions, the solvent molecules can also be incorporated into the cavity of protonated cryptands. For instance, $[H_8L^{13}](ClO_4)_8$ reacts with NaOH in H_2O/MeOH yielding a complex of $[H_4L^{13}(H_2O)(MeOH)]^{4+}$, in which one methanol and one water molecule are simultaneously encapsulated into the cavity of $[H_4L^{13}]^{4+}$.[39] Increasing the pH value to 9, the configuration of $\mathbf{L^{13}}$ is changed, and the encapsulated H_2O and MeOH are released. Tuning the pH value back to 7, H_2O and MeOH are encapsulated again, demonstrating a reversible encapsulation–release process. This result reveals that the encapsulation ability of $\mathbf{L^{13}}$ is pH dependent. It is interesting to find that the quantities and structures of the water clusters within the cavity are affected by the counter-anions around the protonated cryptand. A water dimer and a circular water trimer, a linear water trimer, and a quasi-prismatic hexamer water cluster are encapsulated inside the cavity of $[H_6L^{13}]^{6+}$ using $H_2PO_4^-$, $[CH_3(C_6H_4\text{-}p)SO_3]^-$ and SO_4^{2-} as counter-anions, respectively.[40]

Using heterocyclic spacers such as pyrrole, thiourea and indole instead of an aromatic ring, the recognition abilities and confinements of the resulting cryptands will be greatly enhanced, as introducing these functional groups will provide the cryptands with more hydrogen bonding sites.[41,42] Mani *et al.* systematically investigate the recognition of polyaza cryptands containing pyrrolyl

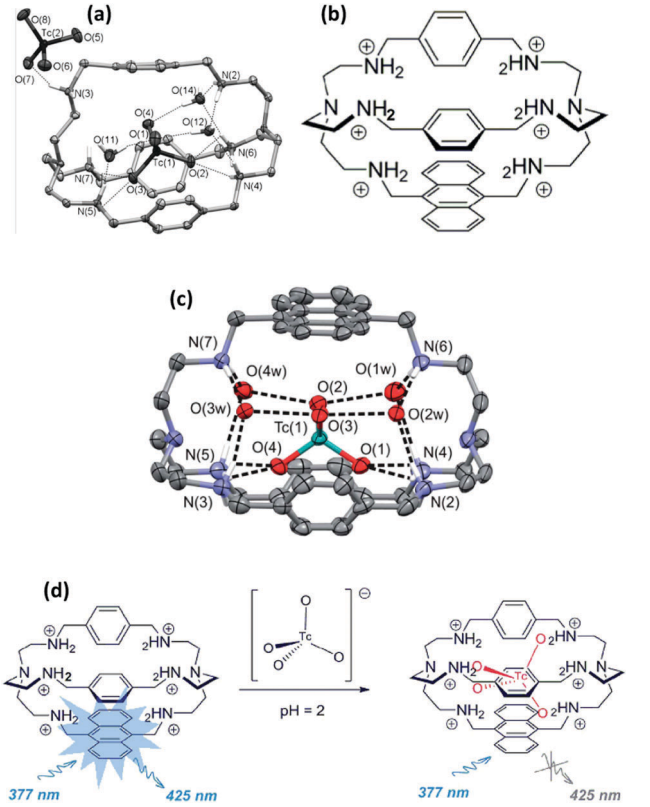


Fig. 14 (a) Crystal structure of $[H_6L^{13}(^{99}TcO_4)](^{99}TcO_4)(CF_3SO_3)_4{\cdot}8H_2O$, (b) chemical structure of $[H_6L^{15}]^{6+}$, and (c) crystal structure of $[H_6L^{15}(^{99}TcO_4)](CF_3SO_3)_5{\cdot}7H_2O$. (d) The formation of an inclusion complex with $^{99}TcO_4^-$ accompanied by quenching the fluorescence of $[H_6L^{15}]^{6+}$.

groups. They prepared a new polyaza cryptand with nitrogen bridgeheads and each spacer containing dipyrrolylmethane subunits by the Mannich reaction ($\mathbf{L^{16}}$, Fig. 15a), and its cavity has a specific size suitable for the recognition of fluoride ions (Fig. 15b); the anion binding studies have shown that $\mathbf{L^{16}}$ has high selectivity and affinity for fluoride ions in acetone over other anions.[43] Then they prepared another hexapyrrolic polyaza cryptand of $\mathbf{L^{17}}$ with long spacers and larger cavity (Fig. 16a). X-ray diffraction analyses have shown that the cavity of $\mathbf{L^{17}}$ is flexible and large enough to encapsulate both smaller fluoride ions and larger oxoanions such as sulfate, phosphate, and arsenate anions (Fig. 16b–d).[44]

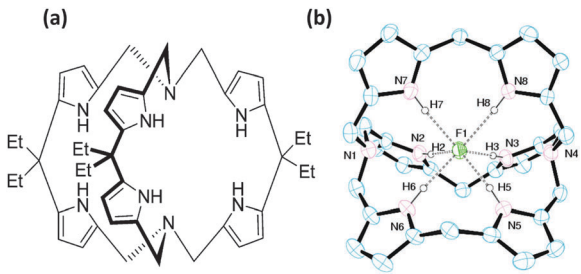


Fig. 15 (a) Chemical structure of $\mathbf{L^{16}}$. (b) Crystal structure of $\mathbf{L^{16}}$ encapsulating with the F^- anion.

This journal is © The Royal Society of Chemistry 2016

Published on 22 June 2016. Downloaded by Library for Natural Sciences of the RAS on 8/27/2018 10:11:04 AM.

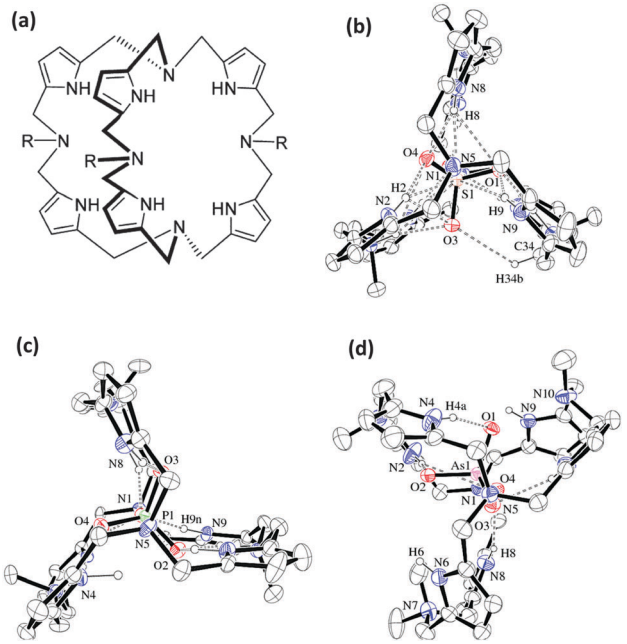


Fig. 16 Chemical structure of L^{17} (a), and crystal structures of L^{17} encapsulating with (b) sulfate (c) phosphate and (d) arsenate anions.

Mani and co-workers further designed and synthesized a hexapyrrolyl polyaza cryptand with bridgehead C atoms by the Mannich reaction of tripyrrolylmethane with primary or secondary amine hydrochloride and formaldehyde (L^{18}, Fig. 17a).[45] The binding studies by ^{1}H NMR titration have shown that L^{18} strongly binds to the F^- anion in DMSO-d_6, with the binding constant beyond 10^4 M^{-1}, greatly higher than those for Cl^- (69 M^{-1}) and Br^- anions (15 M^{-1}). This was supported by the crystal structure results. X-ray diffraction analysis has shown that the F^- anion locates in the cavity center of L^{18} to form an inclusion complex, while Cl^- and Br^- anions locate in the clefts of L^{18} to generate chloride/bromide complexes (Fig. 17b–d). These results show that L^{18} possesses a specific cavity for recognizing the F^- anion.

Using large molecules such as 2,4,6-triethylbenzene as the bridgeheads, the resulting cryptands would possess more rigidity. Mateus *et al.* have synthesized three triethylbenzene-capped macrobicyclic receptors with the spacers slightly changed and systematically studied their anion binding properties (Fig. 18).[46,47] The protonated receptor with *m*-xylyl spacers (L^{19}) has a high selectivity for sulfate in the presence of several monocharged anions,[46] the receptor with pyridyl spacers (L^{20}) has obviously enhanced the affinity for phosphate due to hydrogen bond interactions involving pyridyl N atoms,[47] and the receptor with pyrrolyl spacers (L^{21}) has a very high effective association constant for SO_4^{2-} at pH 4.0 ($\log K_{eff}$ = 6.42), and shows high selectivity for SO_4^{2-} over other anions (Fig. 19). These studies have shown that small structural changes in the receptors can lead to an appreciable impact on the selectivity pattern of the receptors.[48] Roelens *et al.* also investigated the recognition ability of this triethylbenzene-capped macrobicyclic receptor with *m*-xylyl/pyridyl/pyrrolyl spacers. They found that L^{21} exhibits obvious superiority in the binding of β-glucopyranosides compared to

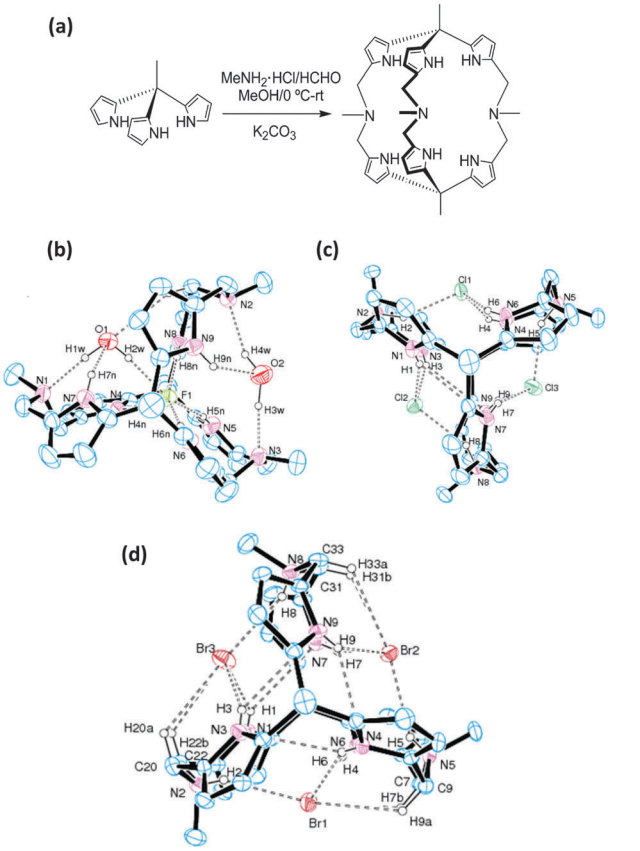


Fig. 17 (a) Synthesis of L^{18}. Crystal structures of (b) $[L^{18}F]^-$, (c) $[H_3L^{18}]Cl_3$, and (d) $[H_3L^{18}]Br_3$.

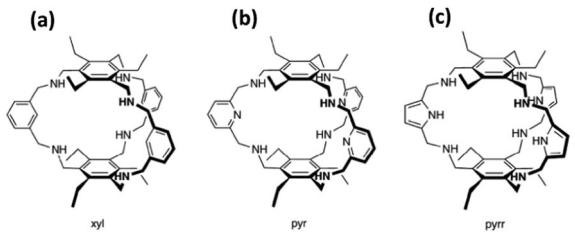


Fig. 18 Triethylbenzene-capped polyaza macrobicycles of (a) L^{19}, (b) L^{20} and (c) L^{21}.

the one with *m*-xylyl/pyridyl spacers, which can be attributed to the hydrogen bonding ability of the pyrrol units.[49]

2.1.3 Polyaza cryptands with asymmetric spacers or bridgeheads. To impart cryptand ligands with specific functions, researchers have tried to design and synthesize macrocyclic ligands containing asymmetric spacers or bridgeheads. This type of host usually contains two different cavities and could be viewed as hetero multianionic receptors that can recognize anions of different dimensions in a single molecular entity. Bharadwaj and co-workers have synthesized two asymmetric cryptands of L^{22} and L^{23} with mixed oxa-aza groups (Fig. 20a and b). In the fluoride complex of L^{22}, the internal fluoride sits above the trigonal plane of the amines, being pulled towards the oxa end by the bridgehead protonated N atom (Fig. 20c and d).[50] In the chloride complex of L^{22}, the encapsulated Cl^- resides

Published on 22 June 2016. Downloaded by Library for Natural Sciences of the RAS on 8/27/2018 10:11:04 AM.

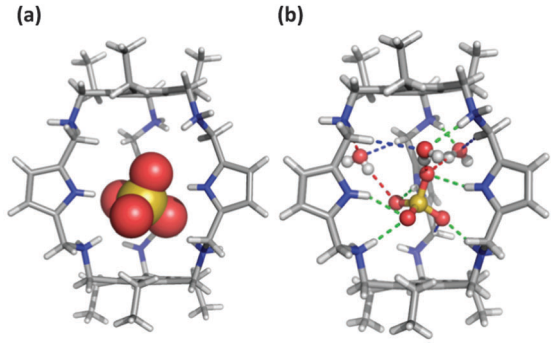


Fig. 19 Crystal structures of $\mathbf{L^{21}}$ encapsulating the SO_4^{2-} anion (a) and the hydrogen bonding interactions between $\mathbf{L^{21}}$ and SO_4^{2-} (b).

perfectly on the C_3 axis and prefers to stay at the oxa end (Fig. 20e).[51] In the bromide complex, $\mathbf{L^{22}}$ changes its conformation and employs a Y-shaped architecture, the Br^- is half-encapsulated in the cavity of the Y-shaped $\mathbf{L^{22}}$ *via* two H-bonds to the secondary amines and one to the bridgehead nitrogen atom (Fig. 20f).[50] Compared with $\mathbf{L^{22}}$, $\mathbf{L^{23}}$ possesses a larger cavity and thus can accommodate not only F^- and Cl^-, but also the whole Br^- within its cavity. The encapsulated $F^-/Cl^-/Br^-$ locates far away from the oxa end and closely to the aza end (Fig. 20g and h). Iodide remains outside the cavity for both cryptands.[50] The investigations of both cryptands for binding nitrate and sulfate anions have also been performed. With a larger cavity, $\mathbf{L^{23}}$ prefers to encapsulate a planar NO_3^- over Td SO_4^{2-} in its cavity in competition experiments. ^{1}H-NMR titration results show that either $[H_3L^{22}]^{3+}$ or $[H_3L^{23}]^{3+}$ binds strongly to SO_4^{2-} and NO_3^-, with the log K values of 4.35 and 4.27 for SO_4^{2-} and 3.12 and 3.13 for NO_3^-, respectively.[52]

Steed *et al.* have synthesized a polyaza cryptand ($\mathbf{L^{24}}$) with different bridgeheads, with one of the bridgehead N atoms replaced with an aromatic ring (Fig. 21a).[53] They have found that the hexaprotonated $\mathbf{L^{24}}$ of $[H_6L^{24}]^{6+}$ exhibits remarkable strong and selective fluoride binding by three N–H···F^- and three C–H···F^- interactions, with the first binding constant of log K_1 as high as 9.54(12). The strong affinity towards F^- can be attributed to the size match between the cavity of $[H_6L^{24}]^{6+}$ and F^- anion. Crystal structure analyses reveal that the average N···F^- distance in $[H_6L^{24}F]^{5+}$ is 2.648 Å (Fig. 21b), suggesting a very good match between the cavity of $[H_6L^{24}]^{6+}$ and the F^- anion. Additionally, the fluoride complex exhibits a rather long anion···centroid separation of 4.506 Å, greatly larger than these in chloride, bromide, and iodide complexes (*ca.* 3.600 Å; Fig. 21c–e), which reduces the repulsive contact between the F^- anion and the aromatic ring, and subsequently reinforces the interaction of $[H_6L^{24}]^{6+}$ with the F^- anion.

Miller and Lu designed an extremely asymmetric macrocyclic ligand ($\mathbf{L^{25}}$, Fig. 22a), in which both the spacers and the bridgeheads are asymmetric. The ligand consists of a triamido-(amine) motif to coordinate the metal ion and a narrow, hydrophobic channel above the metal binding site. The investigation of host–guest chemistry reveals that $[ZnL^{25}]^{2+}$ cannot encapsulate any substrates such as CH_3CN, DMF, and DMSO, hexane, benzene and so on (Fig. 22b). The reason may be that the cavity is so narrow that it would exclude most of the substrates.[54]

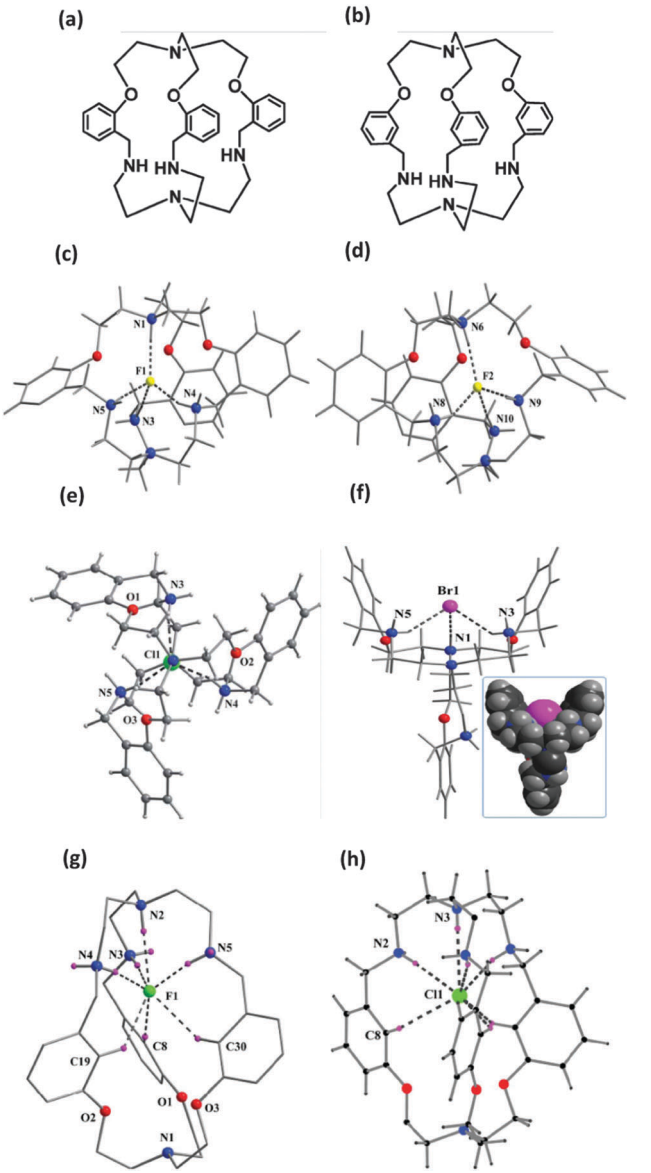


Fig. 20 Chemical structures of (a) $\mathbf{L^{22}}$ and (b) $\mathbf{L^{23}}$. Crystal structures of (c) and (d) $[H_4L^{22}F]^{3+}$, (e) $[H_4L^{22}Cl]^{3+}$, (f) $\{[H_4L^{22}]Br\}^{3+}$, (g) $[H_4L^{23}F]^{3+}$ and (h) $[H_4L^{23}Cl]^{3+}$.

$\mathbf{L^{26}}$ designed by Saha *et al.* is also a polyaza cryptand with both asymmetric spacers and bridgeheads. It contains two distinct cavities consisting of tetra-amine clefts and tri-amide clefts as potential recognition elements for anionic guests (Fig. 23a). Anion binding of protonated $\mathbf{L^{26}}$ to Cl^-, Br^-, ClO_4^- and HSO4$^-$ reveals that the overall association constants show the following order: $HSO_4^- > Br^- > Cl^- \approx ClO_4^-$. Crystal structure analyses show that ClO_4^- is encapsulated in the amide cleft of $[H_2L^{26}]^{2+}$ (Fig. 23b), and Cl^-/Br^- is encapsulated in the ammonium cleft of $[H_3L^{26}]^{3+}$ (Fig. 23c).[55]

2.2 Polyaza cryptates

The polyaza cryptands easily combine two metal ions at two poles to form metal complexes (cryptates), leaving two axial sites vacant and favorable for combining a molecule/anion. The recognition of

 This journal is © The Royal Society of Chemistry 2016

Published on 22 June 2016. Downloaded by Library for Natural Sciences of the RAS on 8/27/2018 10:11:04 AM.

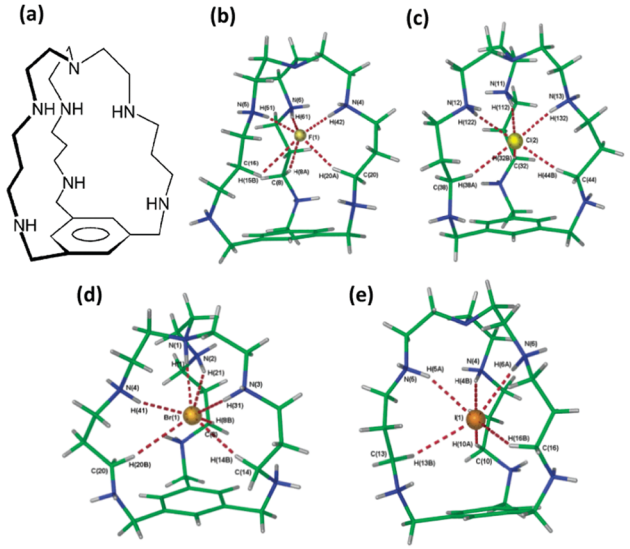


Fig. 21 (a) Molecular structure of $\mathbf{L^{24}}$ and structures of (b) $[H_6L^{24}F]^{5+}$, (c) $[H_6L^{24}Cl]^{5+}$, (d) $[H_6L^{24}Br]^{5+}$, and (e) $[H_6L^{24}I]^{5+}$.

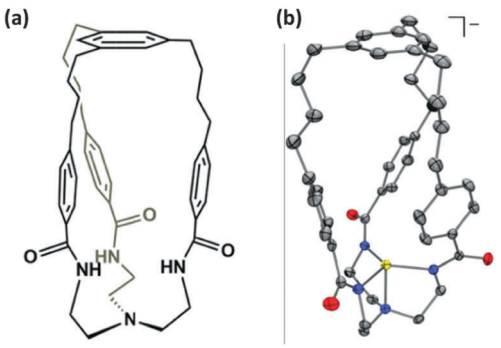


Fig. 22 (a) Chemical structure of $\mathbf{L^{25}}$ and (b) its Zn(II) complex.

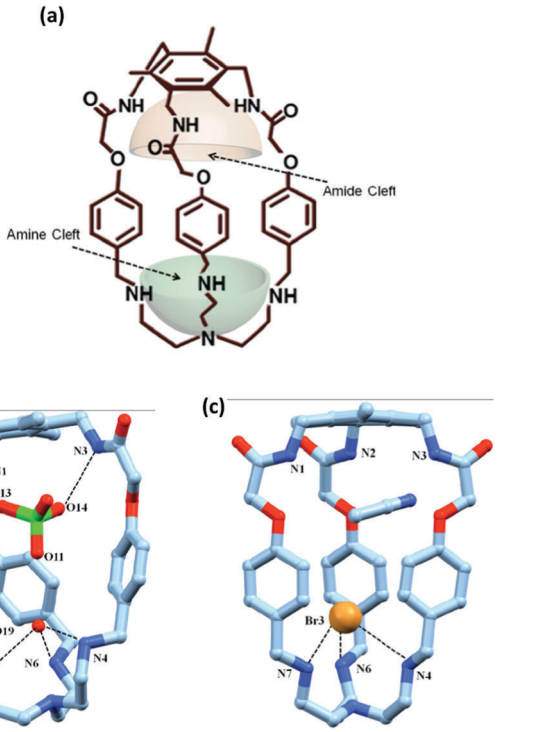


Fig. 23 (a) Chemical structure of $\mathbf{L^{26}}$. Crystal structures of $\mathbf{L^{26}}$ encapsulating (b) ClO_4^- and (c) Br^-.

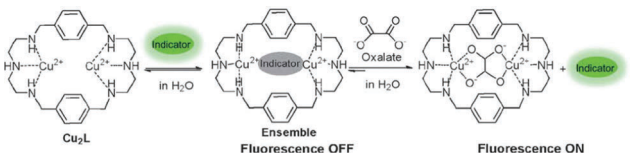


Fig. 24 Complex $[Cu_2L^{27}]^{4+}$ sensing oxalate by indicator-displacement assays.

the resulting dinuclear cryptates to molecules/anions depends on the flexibility and rigidity of the cryptands, as well as the M···M separations. Upon complexation with metal ions, the rigidity of the cryptand ligands will be markedly increased, and the M···M distance will be fixed in a narrow range, which may improve cryptate's selectivity, to recognize an anion with specific size and shape. Hu *et al.* have prepared a dinuclear copper complex of cyclophane ($\mathbf{L^{27}}$, Fig. 24) and investigated its recognition ability towards various dicarboxylates by using indicator-displacement assays. The results have shown that this complex exhibits high selectivity, strong binding affinity and high sensitivity to oxalate in water at neutral pH, which builds a simple but very effective fluorescence sensing system for oxalate.[56] Guillet *et al.* have synthesized a multi-dentate cryptand ($\mathbf{L^{28}}$, Fig. 25a). Combining with iron(III) results in a substantial conformational change of this ligand to give a much rigid trianionic triiron(III) complex of $[K(MeCN)_2]_3[(FeCl_2)_3L^{28}]$ (Fig. 25b).[57]

We have found that the rigid cryptate $[Co_2L^{13}]^{4+}$ can recognize the Cl^- and Br^- rather than F^- and I^-.[58] The Cl^- and Br^- locate at the cavity of $[Co_2L^{13}]^{4+}$ and bridge two Co(II) to form two cascade complexes of $[Co_2L^{13}Cl]^{3+}$ and $[Co_2L^{13}Br]^{3+}$ (Fig. 26a), with the association constants ($\log K$) of 5.7(1) and 5.2(1), respectively. The F^- is too small to form an F^- bridged cryptate, while the I^- is too large to be encapsulated inside the cryptate cavity. Instead, the I^- locates outside the cavity as a counteranion to form a complex of $[Co_2L^{13}(OH)(H_2O)]^{3+}$, in which the two axial positions of two Co(II) are occupied by a water molecule and an OH^-, respectively (Fig. 26b). $[Co_2L^{14}]^{4+}$ can also recognize Cl^- to form $[Co_2L^{13}Cl]^{3+}$ (Fig. 26c), with the association constant ($\log K$) of 4.2(1). This value is smaller than that of $[Co_2L^{13}Cl]^{3+}$, indicating that the stability of $[Co_2L^{13}Cl]^{3+}$ is higher than that of $[Co_2L^{14}Cl]^{3+}$ due to the rigid conformation of $\mathbf{L^{13}}$. The binuclear metal complex of $\mathbf{L^{13}}$ can also recognize organic anions. For instance, $[Cu_2L^{13}]^{4+}$ can bind the imidazolate (Im^-) anion within its cavity to form a sandwich-like dinuclear cryptate $[Cu_2L^{13}(Im)]^{3+}$ (Fig. 26d).[59]

Elongating the spacers, the cavity of the resulting crytands will enlarge, which can combine longer substrates.[60] Mateus *et al.* prepared a cryptand of $\mathbf{L^{29}}$ with biphenylmethane spacers (Fig. 27a), and its dinuclear copper(II) complex can recognize longer dicarboxylate anions such as adipate (adi) and terephthalate (tph) (Fig. 27b and c).[60a] Polyaza macrobicycles with different

Published on 22 June 2016. Downloaded by Library for Natural Sciences of the RAS on 8/27/2018 10:11:04 AM.

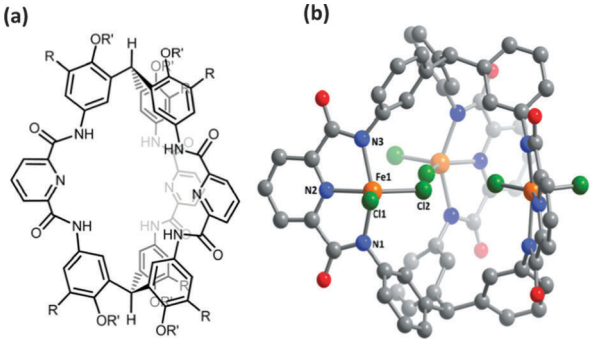


Fig. 25 (a) Chemical structure of L^{28}. (b) A portion of the crystal structure of $[K(MeCN)_2]_3[(FeCl_2)_3L^{28}]$.

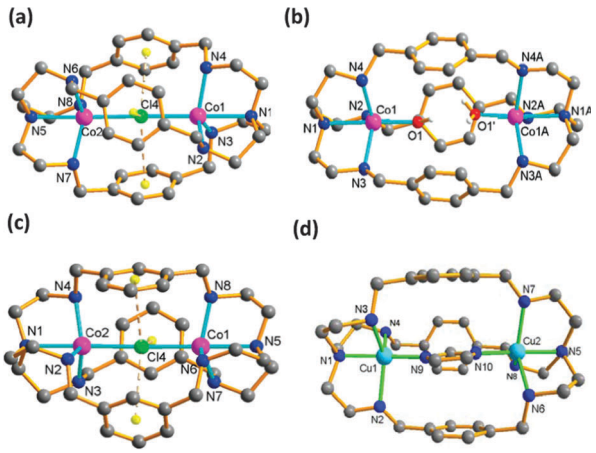


Fig. 26 Crystal structures of (a) $[Co_2L^{13}Cl]^{3+}$, (b) $[Co_2L^{13}(OH)(H_2O)]^{3+}$, (c) $[Co_2L^{14}Cl]^{3+}$, and (d) $[Cu_2L^{13}(Im)]^{3+}$.

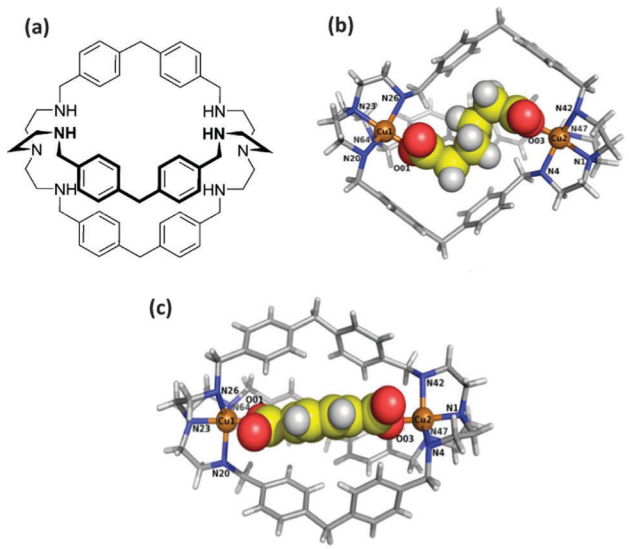


Fig. 27 (a) Chemical structure of L^{29}. Crystal structures of (b) $[Cu_2L^{29}$-$(\mu\text{-adi})]^{2+}$ and (c) $[Cu_2L^{29}(\mu\text{-tph})]^{2+}$.

bridgeheads can also combine metal ions to form cryptate, which can further recognize other anions at the axial position. For instance, Mateus *et al.* synthesized a heteroditopic cryptand L^{30},

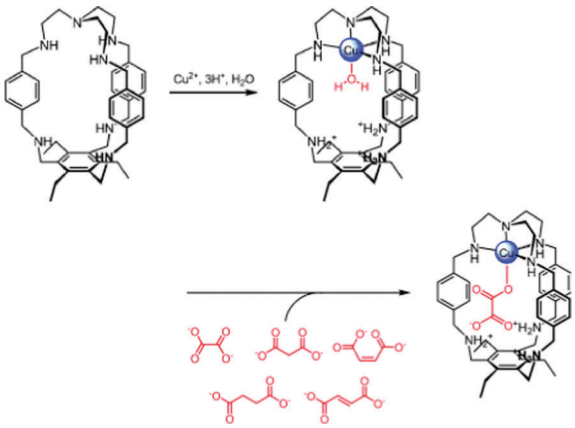


Fig. 28 Cu(II) capsule based on polyaza cryptand with different bridgeheads and its selective binding with the oxalate anion.

in which one head is appropriate for the coordination of Cu(II), whereas the other head is available for additional hydrogen-bonding and electrostatic interactions with substrates (Fig. 28). They found that this Cu(II) capsule bound to the oxalate anion more strongly than malate, succinate and fumarate anions in aqueous solutions.[61]

3. Recognition of polyaza macrotricycles with tetrahedral caged geometries

Polyaza macrotricycles allow for even larger cavities, which can encapsulate more complex or larger anionic guests. In this field, Cooper and co-workers have done systematic research work. They have synthesized several organic tetrahedral cages by a simple condensation reaction of C_3 trialdehydes (*e.g.* 1,3,5-triformylbenzene) and 1,2-substituted vicinal diamines (*e.g.* ethylenediamine and (*R*,*R*)-1,2-diaminocyclohexane) (Fig. 29a). They studied the selectivity of these cages to C_8 and C_9 aromatic molecules (*e.g.* xylenes and mesitylene and its isomers) in four different ways,

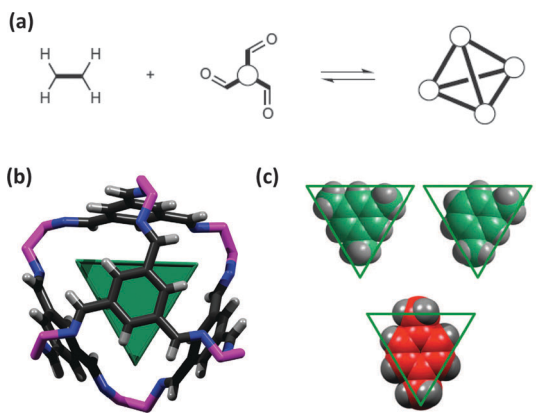


Fig. 29 (a) Synthesis of organic cages. (b) Structure of organic tetrahedral cages L^{31}, the triangular cavity in the cage (highlighted in green) is a good shape match for (c) mesitylene, and *m*-xylene, but not for *p*-xylene.

This journal is © The Royal Society of Chemistry 2016

Published on 22 June 2016. Downloaded by Library for Natural Sciences of the RAS on 8/27/2018 10:11:04 AM.

including molecular simulations, solution-phase binding studies, sorption experiments, and molecular dynamics simulations.[62] They found that organic cage **L**[31] can separate organic molecules by size and shape. The 1,3,5-substituted aromatic cage in **L**[31] generates a cavity with a three-fold axis of symmetry. Both *meta*-xylene (mX) and mesitylene (Mes) have 1,3-substituted geometries that can match this cavity geometry which can be encapsulated into its cavity, whereas *para*-xylene (pX) does not match, thus cannot be encapsulated into the cavity (Fig. 29b and c).

Cooper's group have also synthesized a series of porous covalent organic tetrahedral cages by the Schiff base condensation reactions of triformyl-compounds with diamine-compounds (Fig. 30a and b).[63] Gas sorption investigations have revealed that these porous organic cages show highly selective adsorption of sulfur hexafluoride (SF_6) over nitrogen (Fig. 30c and d). Their superior SF_6/N_2 selectivity can be rationalized by the cooperative diffusion and structural rearrangements in these molecular crystals. They also show unprecedented performance in the solid state for the separation of rare gases, such as krypton and xenon (Fig. 30e). The selectivity arises from a precise size match between the rare gas and the organic cage cavity, as predicted by molecular simulations. Additionally, these porous cage molecules also show promising application in chiral separation, and for selective binding of chiral organic molecules such as 1-phenylethanol (Fig. 30f).[64]

Bowman-James *et al.* synthesized an amine/amide mixed covalent organic tetrahedral cage **L**[32] using tris(2-aminoethyl)-amines (tren) as bridgeheads and 2,6-diacetylpyridine units as linkers (Fig. 31a).[65] The cage **L**[32] contains 12 amide NH groups plus four tertiary amine N groups, the latter of which are positioned in a pseudo-tetrahedral array. Host–guest chemistry investigations have shown that **L**[32] can encapsulate the DMF molecule (Fig. 31b), the $[H_2O{\cdot}4H_2O]$ cluster (Fig. 31c), as well as the $[F^-{\cdot}4H_2O]$ cluster (Fig. 31d).

4. Activation of the substrate by polyaza macrocyclic ligands and their complexes

Activation of covalent bonds is a key process in organic and organometallic synthetic chemistry. Supramolecular receptors bearing appropriate binding sites may act like enzymes to activate and transform the substrate into the product under mild conditions. This process usually involves two steps: one is the recognition of a substrate by a receptor, and the other is the transformation of the bound substrate to product. Polyaza macrocyclic ligands and their metal complexes, as one class of the most important receptors in host–guest chemistry, not only show recognition of molecules and anions, but also exhibit activation to the capsulated molecules and anions to some extent.

Nocera *et al.* have found that hexacarboxamide cryptand **L**[33] (Fig. 32a) can encapsulate the O_2^{2-} dianion generated from the disproportionation of potassium superoxide or reduced of O_2 by cobaltocene, to form $[(O_2)L^{33}]^{2-}$ at room temperature in

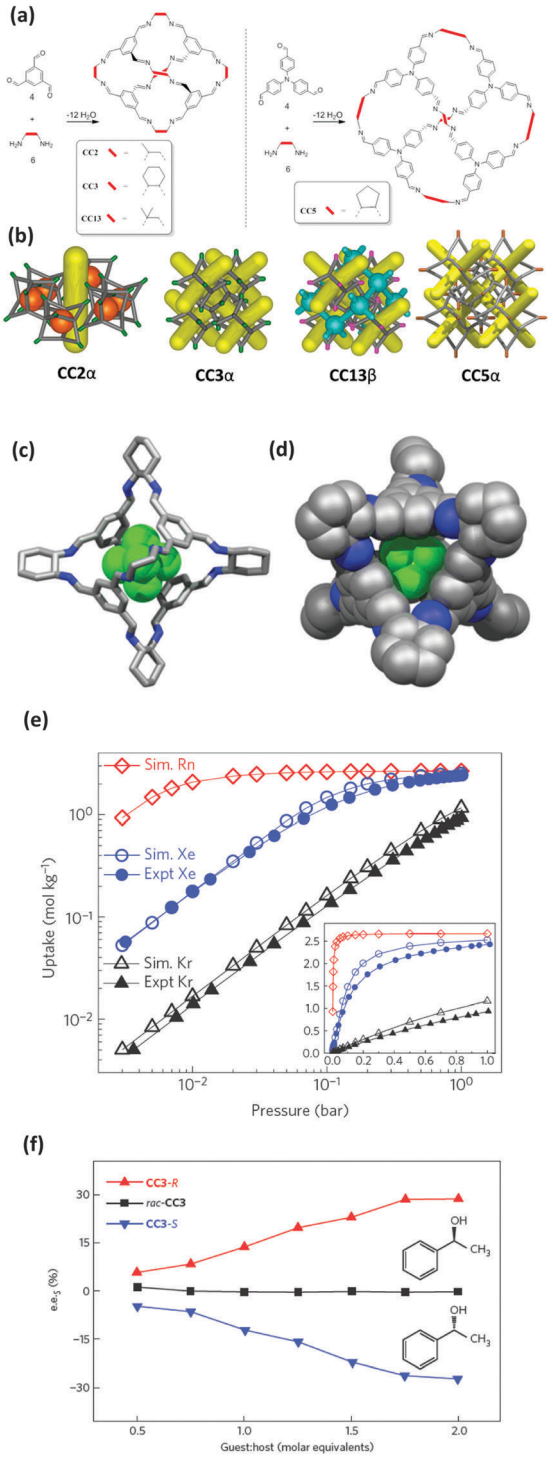


Fig. 30 (a) Synthesis and structure of organic cages. (b) Simplified structural representations of the packing and porosity of these cages as derived from single crystal structures. (c and d) Position of SF_6 in the cage cavity drawn from the single crystal structure. (e) Predicted single-component log–log gas adsorption isotherms (Kr, Xe and Rn; open symbols) and experimental equivalents (Kr, Xe; filled symbols) at 298 K for CC3 (inset shows linear–linear plot). (f) Measured enantiomeric excess of the *S* enantiomer of 1-phenylethanol adsorbed in cages over a range of guest/host ratios.

dimethyl sulfoxide (DMSO) and *N*,*N*′-dimethylformamide (DMF). The result of X-ray diffraction analysis indicates that

Published on 22 June 2016. Downloaded by Library for Natural Sciences of the RAS on 8/27/2018 10:11:04 AM.

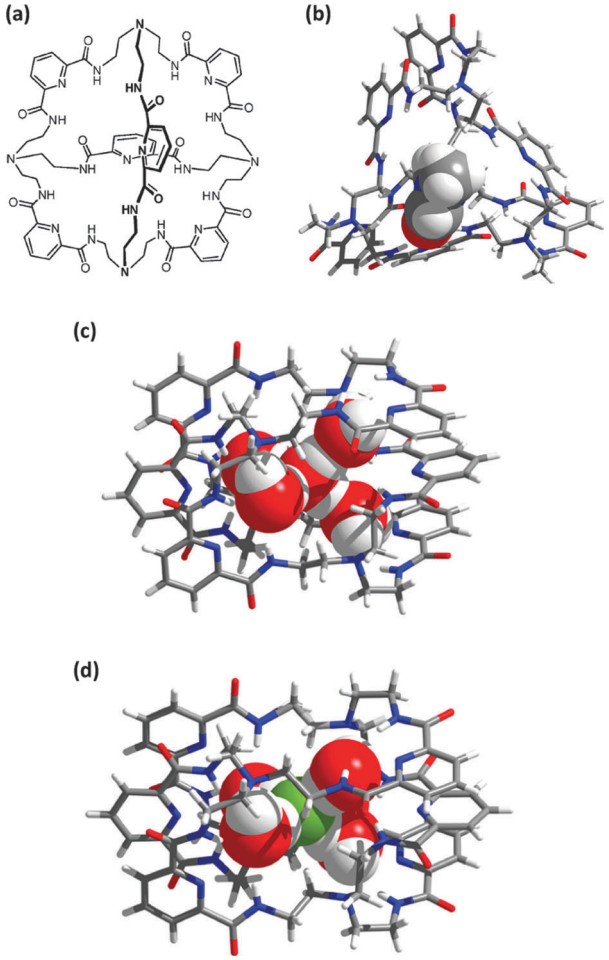


Fig. 31 (a) Chemical structure of $\mathbf{L^{32}}$. Crystal structures of $\mathbf{L^{32}}$ incorporated with (b) DMF, (c) $[H_2O{\cdot}4H_2O]$ cluster, and (d) $[F^-{\cdot}4H_2O]$ cluster.

the O_2^{2-} dianion is stabilized by strong hydrogen bonds with N–H groups from $\mathbf{L^{33}}$ (Fig. 32b).[66] They have further found that the encapsulated peroxide cryptate, $[(O_2)L^{33}]^{2-}$, can react with carbon monoxide in organic solvents at 40 °C to efficiently form an encapsulated carbonate, $[(CO_3)L^{33}]^{2-}$ (Fig. 32c).[67] Single crystal X-ray diffraction has revealed that there are nine complementary hydrogen bonds between $\mathbf{L^{33}}$ and CO_3^{2-}, which is also supported by spectroscopic data. Labeling studies and ^{17}O solid-state NMR data have further confirmed that two-thirds of the oxygen atoms in the encapsulated CO_3^{2-} derive from the peroxide dianion, and the carbon is fully derived from CO. This work demonstrates a creative method for CO oxidation, realized by a hydrogen bonding anion receptor.

Besides being oxidized from CO, the CO_3^{2-}-based cryptate adducts can also be formed by directly taking up atmospheric CO_2. Reaction of Cu(II) with cryptand $\mathbf{L^{14}}$ (Fig. 11b) has not afforded an expected binuclear Cu(II) product of $[Cu_2L^{14}]^{4+}$, instead, a μ-O_2COH^- bridged cryptate of $[Cu_2L^{14}(\mu\text{-}O_2COH)]^{3+}$ has been formed within a few minutes. Nelson and co-workers presumed that the generation of $O_2COCH_3^-$ by $[Cu_2L^{14}]^{4+}$ in methanol may follow a mechanism of CO_2 insertion into the M–OCH_3 bond.[68] Further systematic investigation on this reaction

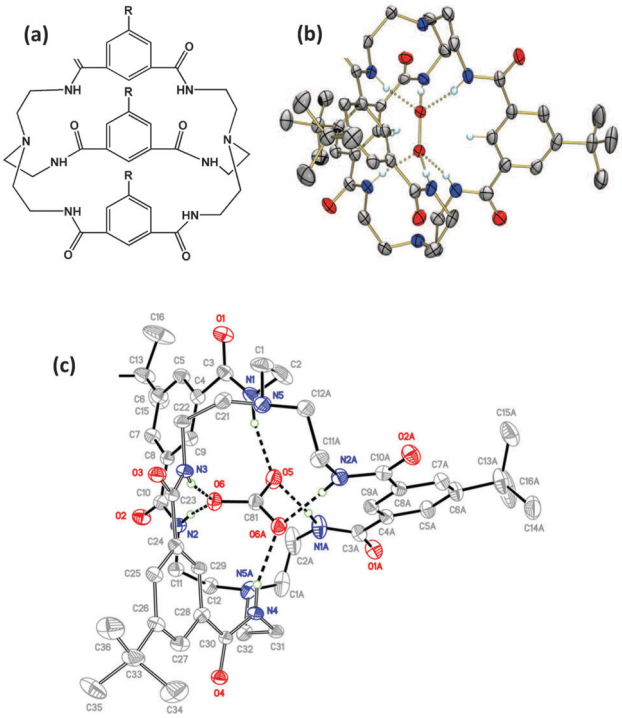


Fig. 32 Chemical structure of $\mathbf{L^{33}}$ (a), and crystal structures of (b) $[(O_2)L^{33}]^{2-}$ and (c) $[(CO_3)L^{33}]^{2-}$.

indicates that alkyl carbonate formation does not result from CO_2 insertion into the M–OCH_3 bond. Instead, the cryptate $[Cu_2L^{14}]^{4+}$ can readily absorb the atmospheric CO_2 even under acidic conditions to form μ-O_2COH^- bridged cryptate $[Cu_2L^{14}(\mu\text{-}O_2COH)]^{3+}$, which can be efficiently transformed to alkylcarbonate in alcohol solutions (Fig. 33).[69]

Other polyaza macrocyclic ligands have also found the capacity of immobilizing atmospheric CO_2. Bowman-James's group designed a 24-membered diamine-tetraamido macrocycle ($\mathbf{L^{34}}$), which has been found to react with CO_2 rapidly and efficiently, with 100% conversion within 1 min at room temperature (Fig. 34a).[70] Compared with the general observation that the rapid uptake of CO_2 by amine-containing systems is often readily released, the process for CO_2 release from $\mathbf{L^{34}}$ requires heating to 100 °C, showing extremely strong affinity between $\mathbf{L^{34}}$ and CO_2 molecules.

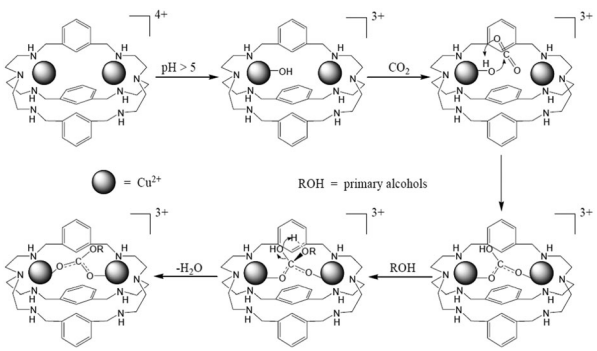


Fig. 33 Proposed formation mechanism of alkylcarbonate within $[Cu_2L^{14}]^{4+}$.

This journal is © The Royal Society of Chemistry 2016

Published on 22 June 2016. Downloaded by Library for Natural Sciences of the RAS on 8/27/2018 10:11:04 AM.

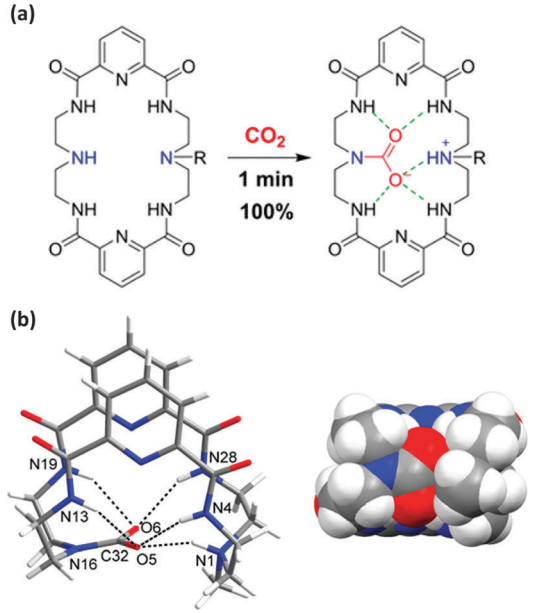


Fig. 34 (a) Rapid reaction of $\mathbf{L^{34}}$ with bubbling CO_2. (b) Crystal structure of $\mathbf{L^{34}}$ loaded with CO_2.

Single crystal X-ray diffraction analyses have shown that CO_2 molecules are apparently tightly bound by a "macrocyclic effect", including multiple well-placed hydrogen bonds and an electrostatic zwitterionic interaction (Fig. 34b).

It is interesting to note that using $\mathbf{L^{13}}$ (Fig. 11a) instead of $\mathbf{L^{14}}$ (Fig. 11b), the resulting dinuclear Cu(II) cryptates show different reactivity. Dissolved in acetonitrile, $[Cu_2L^{13}]^{4+}$ does not adsorb atmospheric CO_2 to form a μ-O_2COH^- bridged cryptate of $[Cu_2L^{13}(\mu\text{-}O_2COH)]^{3+}$, instead, a cyano-bridged dinuclear cryptate $[Cu_2L^{13}(CN)]^{3+}$ is generated (Fig. 35a). We have systematically investigated this reaction and concluded that dinuclear cryptate $[Cu_2L^{13}]^{4+}$ can cleave the C–C bond of acetonitrile at room temperature to produce a cyano-bridged dinuclear cryptate $[Cu_2L^{13}(CN)]^{3+}$ and methanol, due to the strong recognition between the receptor and the substrate (cyanide anion).[71] The observed rate constant

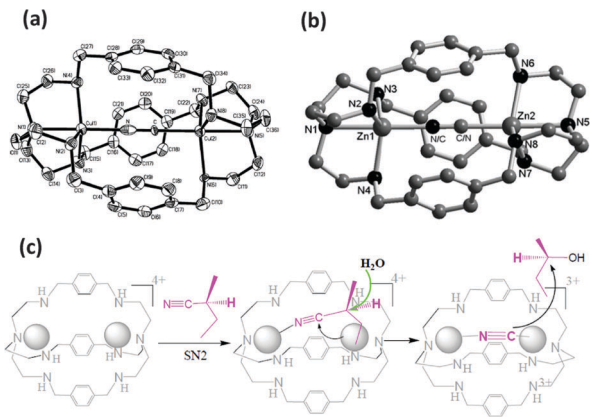


Fig. 35 Crystal structures of (a) $[Cu_2L^{13}(CN)]^{3+}$ and (b) $[Zn_2L^{13}(CN)]^{3+}$. (c) S_N2 reaction pathway within C–C bond cleavage of nitriles by dinuclear Cu(II)/Zn(II) cryptate with L^{13}.

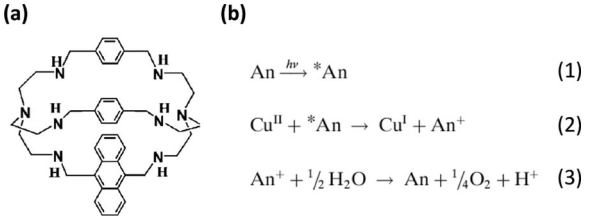


Fig. 36 (a) Chemical structure of $\mathbf{L^{35}}$. (b) Possible reaction mechanism of water oxidation catalyzed by photo-active $\mathbf{L^{35}}$ (An = anthracene).

and half time, determined spectrophotometrically, are 1.52×10^{-4} s^{-1} and 76 min, respectively. Further investigations[72] indicate that the dinuclear zinc(II) cryptate $[Zn_2L^{13}]^{4+}$ can also cleave the C–C bond of nitriles including acetonitrile, propionitrile and benzonitrile at room temperature, resulting in the cyano-bridged cryptate $[Zn_2L^{13}(CN)]^{3+}$ (Fig. 35b) and corresponding alcohol. The observed rate constant and half time are 3.0×10^{-4} s^{-1} and 39 min, respectively, indicating that the cleavage rate for $[Zn_2L^{13}]^{4+}$ is faster than that of $[Cu_2L^{13}]^{4+}$. The HPLC measurements have shown that the C–C bond cleavage of (*S*)-(+)-2-methylbutyronitrile by $[Zn_2L^{13}]^{4+}$ produces (*R*)-(−)-2-butanol only, revealing that the cleavage reaction proceeds through an S_N2 pathway (Walden inversion) (Fig. 35c).

Considering many organic ligands containing an anthracene (An) fragment can be used for fluorescent switches, we introduced an anthracene spacer to replace one aromatic spacer of L^{13}. The resulting polyaza cryptand $\mathbf{L^{35}}$ is endowed with photo-active properties (Fig. 36a). We found that by this fluorescently active $\mathbf{L^{35}}$, the photocatalytic reductive reaction of Cu(II) to Cu(I) in acetonitrile can be realized. In the reaction system, the H_2O molecule serves as a sacrificial electron donor and is oxidized to O_2, which has been evidenced by $H_2{}^{18}O$ labeling studies.[73] The possible reaction mechanism is that an electron is firstly excited from the ground state of the An fragment in $[H_6L^{35}]^{6+}$ to its excited state *An under light irradiation (eqn (1)). The electron in the exited-state *An moiety is then transferred to Cu(II) to generate Cu(I) and an An^+ cation (eqn (2)). Finally, the An^+ cation gains an electron from water to form An, and water is oxidized to oxygen (eqn (3)) (Fig. 36b). Recently, we developed another nickel-based robust homogeneous water oxidation catalyst (WOC), $[Ni(meso\text{-}L^{10})](ClO_4)_2$,[26] which can electrocatalyze water oxidation in phosphate buffer at neutral pH. The overpotential is as low as 170 mV, much lower than the typical overpotentials for many homogeneous WOCs (300–600 mV).[74]

Conclusions and outlook

This review presents the recent works on the recognition of molecules and anions by polyaza macrocycles, macrobicycles and macrotricycles, as well as the activation of molecules and anions by polyaza macrocyclic ligands and their metal complexes. These works evidence the rapid development of the host–guest chemistry during the past several decades. Obviously, with the development of the macrocyclic chemistry, the host molecules have become more and more structurally complicated and functionally

Published on 22 June 2016. Downloaded by Library for Natural Sciences of the RAS on 8/27/2018 10:11:04 AM.

specific, and substrate recognization has extended from simple anions such as X^-, NO_3^-, SO_4^{2-} to large organic molecules/anions such as terephthalate and isophthalate. As the size of the cavities and the functional group within the ligands mostly determine the functions of macrocyclic compounds, the delicate designs for the hosts are very important to develop macrocyclic ligands with super-specific molecular recognition abilities. A change or modification of the spacers or bridgeheads is a universal method to obtain functional macrocyclic hosts, which will not only tune the cavity size of macrocyclic ligands, but also introduce functional groups into the macrocyclic ligands. Therefore, in future, more and more efforts should be devoted to precisely designing hosts according to the requirements of the substrate molecules. Additionally, due to the confinement of the cavity and multi-hydrogen bond interactions, polyaza macrocyclic ligands have shown superiority in the encapsulation of unstable molecules or anions, which may provide a promising research direction for polyaza macrocyclic compounds as reaction media in the future.

Acknowledgements

This work was financially supported by the 973 program of China (2014CB845602), the National Natural Science Foundation of China (21331007, 21363001 and 21401026), and Major Project for Science and Technology of Jiangxi Province (20152ACB21016).

Notes and references

1 C. C. Gillispie, *Dictionary of Scientific Biography*, Scribner, New York, 1975.
2 A. M. Silverstein, *Nat. Immunol.*, 2001, **2**, 279.
3 K. Bowman-James, *Acc. Chem. Res.*, 2005, **38**, 671.
4 (*a*) H. J. Schneider and A. K. Yatsimirsky, *Chem. Soc. Rev.*, 2008, **37**, 263; (*b*) V. Amendola, M. Bonizzoni, D. Esteban-Gómez, L. Fabbrizzi, M. Licchelli, F. Sancenón and A. Taglietti, *Coord. Chem. Rev.*, 2006, **250**, 1451.
5 (*a*) H. Sun, C. A. Hunter and E. M. Llamas, *Chem. Sci.*, 2015, **6**, 1444; (*b*) S. Brahma, S. A. Ikbal, A. Dhamija and S. P. Rath, *Inorg. Chem.*, 2014, **53**, 2381.
6 (*a*) F. P. Schmidtchen, *Chem. Soc. Rev.*, 2010, **39**, 3916; (*b*) K. Tahara, S. B. Lei, J. Adisoejoso, S. De Feyter and Y. Tobe, *Chem. Commun.*, 2010, **46**, 8507.
7 (*a*) C. Talotta, C. Gaeta, Z. Qi, C. A. Schalley and P. Neri, *Angew. Chem., Int. Ed.*, 2013, **52**, 7437; (*b*) M. M. Safont-Sempere, G. Fernández and F. Würthner, *Chem. Rev.*, 2011, **111**, 5784.
8 (*a*) A. F. Hirschbiel, B. V. K. J. Schmidt, P. Krolla-Sidenstein, J. P. Blinco and C. Bamer-Kowollik, *Macromolecules*, 2015, **48**, 4410; (*b*) F. van de Manakker, T. Vermonden, C. F. van Nostrum and W. E. Hennink, *Biomacromolecules*, 2009, **10**, 3157.
9 E. Burda and J. Rademann, *Nat. Commun.*, 2014, **5**, 5170.
10 (*a*) K. Ariga, H. Ito, J. P. Hill and H. Tsukube, *Chem. Soc. Rev.*, 2012, **41**, 5800; (*b*) B. Zheng, F. Wang, S. Y. Dong and F. H. Huang, *Chem. Soc. Rev.*, 2012, **41**, 1621.
11 (*a*) D. S. Kim and J. L. Sessler, *Chem. Soc. Rev.*, 2015, **44**, 532; (*b*) D. S. Guo and Yu. Liu, *Acc. Chem. Res.*, 2014, **47**, 1925; (*c*) D. S. Guo and Yu. Liu, *Chem. Soc. Rev.*, 2012, **41**, 5907; (*d*) M. X. Wang, *Acc. Chem. Res.*, 2012, **45**, 182; (*e*) C. H. Lee, H. Miyaji, D. W. Yoon and J. L. Sessler, *Chem. Commun.*, 2008, 24; (*f*) P. Anzenbacher Jr., R. Nishiyabu and M. A. Palacios, *Coord. Chem. Rev.*, 2006, **250**, 2929; (*g*) J. L. Sessler, S. Camiolo and P. A. Gale, *Coord. Chem. Rev.*, 2003, **240**, 17; (*h*) P. A. Gale, P. Anzenbacher Jr. and J. L. Sessler, *Coord. Chem. Rev.*, 2001, **222**, 57.
12 (*a*) S. J. Barrow, S. Kasera, M. J. Rowland, J. del Barrio and O. A. Scherman, *Chem. Rev.*, 2015, **115**, 12320; (*b*) K. I. Assaf and W. M. Nau, *Chem. Soc. Rev.*, 2015, **44**, 394; (*c*) L. P. Cao, M. Sekutor, P. Y. Zavalij, K. Mlinaric-Majerski, R. Glaser and L. Isaacs, *Angew. Chem., Int. Ed.*, 2014, **53**, 988.
13 (*a*) G. Yu, K. Jie and F. H. Huang, *Chem. Rev.*, 2015, **115**, 7240; (*b*) K. Jie, Y. Zhou, Y. Yao, B. Shi and F. H. Huang, *J. Am. Chem. Soc.*, 2015, **137**, 10472; (*c*) P. J. Cragg and K. Sharma, *Chem. Rev.*, 2012, **41**, 597.
14 (*a*) S. Dong, B. Zheng, F. Wang and F. H. Huang, *Acc. Chem. Res.*, 2014, **47**, 1982; (*b*) P. A. Vigato, V. Peruzzo and S. Tamburini, *Coord. Chem. Rev.*, 2012, **256**, 953; (*c*) P. Ballester, *Chem. Soc. Rev.*, 2010, **39**, 3810; (*d*) S. O. Kang, J. M. Llinares, V. W. Day and K. Bowman-James, *Chem. Soc. Rev.*, 2010, **39**, 3980.
15 (*a*) T. Ren, *Chem. Commun.*, 2016, **52**, 3271; (*b*) X. Liang and P. J. Sadler, *Chem. Soc. Rev.*, 2004, **33**, 246; (*c*) M. Meyer, V. Dahaoui-Gindrey, C. Lecomte and R. Guilard, *Coord. Chem. Rev.*, 1998, **178–180**(Part 2), 1313; (*d*) E. Kimura, *Tetrahedron*, 1992, **48**, 6175; (*e*) K. P. Wainwright, *Coord. Chem. Rev.*, 1997, **166**, 35; (*f*) W. Radecka-Paryzek, V. Patroniak and J. Lisowski, *Coord. Chem. Rev.*, 2005, **249**, 2156; (*g*) J. M. Llinares, D. Powell and K. Bowman-James, *Coord. Chem. Rev.*, 2003, **240**, 57; (*h*) F. P. Schmitchen and M. Berger, *Chem. Rev.*, 1997, **97**, 1609; (*i*) A. Bencini, A. Bianchi, P. Paoletti and P. Paoli, *Coord. Chem. Rev.*, 1992, **120**, 51; (*j*) C. A. Ilioudis and J. W. Steed, *J. Supramol. Chem.*, 2001, **1**, 165.
16 S. O. Kang, M. A. Hossain and K. Bowman-James, *Coord. Chem. Rev.*, 2006, **250**, 3038.
17 G. Mani, D. Jana, R. Kumar and D. Ghorai, *Org. Lett.*, 2010, **12**, 3212.
18 G. Mani, T. Guchhait, R. Kumar and S. Kumar, *Org. Lett.*, 2010, **12**, 3910.
19 R. Kumar, T. Guchhait and G. Mani, *Inorg. Chem.*, 2012, **51**, 9029.
20 H. Zhou, Y. Zhao, G. Gao, S. Li, J. Lan and J. You, *J. Am. Chem. Soc.*, 2013, **135**, 14908.
21 Q. H. Guo, L. Zhao and M. X. Wang, *Angew. Chem., Int. Ed.*, 2015, **54**, 8386.
22 J. S. Mendy, M. A. Saeed, F. R. Fronczek, D. R. Powell and M. A. Hossain, *Inorg. Chem.*, 2010, **49**, 7223.
23 M. Zhang, W. J. Ma, C. T. He, L. Jiang and T. B. Lu, *Inorg. Chem.*, 2013, **52**, 4873.
24 L. G. Warner, N. J. Rose and D. H. Busch, *J. Am. Chem. Soc.*, 1967, **89**, 703.
25 B. J. Fisher and R. Eisenberg, *J. Am. Chem. Soc.*, 1980, **102**, 7361.
26 M. Zhang, M. T. Zhang, C. Hou, Z. F. Ke and T. B. Lu, *Angew. Chem., Int. Ed.*, 2014, **53**, 13042.
27 G. C. Ou, L. Jiang, X. L. Feng and T. B. Lu, *Inorg. Chem.*, 2008, **47**, 2710.
28 H. Y. Li, L. Jiang, H. Xiang, T. A. Makal, H. C. Zhou and T. B. Lu, *Inorg. Chem.*, 2011, **50**, 3177.
29 G. C. Ou, L. Jiang, X. L. Feng and T. B. Lu, *Cryst. Growth Des.*, 2011, **11**, 851.
30 B. Dietrich, J. M. Lehn, J. Guilhem and C. Pascard, *Tetrahedron Lett.*, 1989, **30**, 4125.
31 M. A. Hossain, J. M. Llinares, C. A. Miller, L. Seib and K. Bowman-James, *Chem. Commun.*, 2000, 2269.
32 M. Arunachalam, E. Suresh and P. Ghosh, *Tetrahedron*, 2007, **63**, 11371.
33 R. J. Motekaitis, A. E. Martell, I. Murase, J. M. Lehn and M. W. Hosseini, *Inorg. Chem.*, 1988, **27**, 3630.
34 P. S. Lakshminarayanan, I. Ravikumar, E. Suresh and P. Ghosh, *Cryst. Growth Des.*, 2008, **8**, 2842.
35 L. Z. Yang, Y. Li, L. Jiang, X. L. Feng and T. B. Lu, *CrystEngComm*, 2009, **11**, 2375.
36 O. S. Kang, A. M. Hossain, D. Powell and K. Bowman-James, *Chem. Commun.*, 2005, 328.
37 R. Alberto, G. Bergamaschi, H. Braband, T. Fox and V. Amendola, *Angew. Chem., Int. Ed.*, 2012, **51**, 9772.
38 V. Amendola, G. Bergamaschi, M. Boiocchi, R. Alberto and H. Braband, *Chem. Sci.*, 2014, **5**, 1820.
39 L. Z. Yang, L. Jiang, X. L. Feng and T. B. Lu, *CrystEngComm*, 2008, **10**, 649.
40 Y. Li, L. Jiang, X. L. Feng and T. B. Lu, *Cryst. Growth Des.*, 2008, **8**, 3689.
41 M. Arunachalam and P. Ghosh, *Chem. Commun.*, 2011, **47**, 8477.
42 P. Ballester, *Chem. Soc. Rev.*, 2010, **39**, 3810.
43 T. Guchhait and G. Mani, *J. Org. Chem.*, 2011, **76**, 10114.
44 D. Jana, G. Mani and C. Schulzke, *Inorg. Chem.*, 2013, **52**, 6427.
45 T. Guchhait, G. Mani, C. Schulzke and A. Anoop, *Inorg. Chem.*, 2012, **51**, 11635.

 This journal is © The Royal Society of Chemistry 2016

Published on 22 June 2016. Downloaded by Library for Natural Sciences of the RAS on 8/27/2018 10:11:04 AM.

46 P. Mateus, R. Delgado, P. Brandão, S. Carvalho and V. Félix, *Org. Biomol. Chem.*, 2009, **7**, 4661.
47 P. Mateus, R. Delgado, P. Brandão and V. Félix, *J. Org. Chem.*, 2009, **74**, 8638.
48 P. Mateus, R. Delgado, V. André and M. T. Duarte, *Org. Biomol. Chem.*, 2015, **13**, 834.
49 O. Francesconi, M. Gentili and S. Roelens, *J. Org. Chem.*, 2012, **77**, 7548.
50 M. C. Das, S. K. Ghosh and P. K. Bharadwaj, *Dalton Trans.*, 2009, 6496.
51 M. C. Das, S. K. Ghosh, S. Sen and P. K. Bharadwaj, *CrystEngComm*, 2010, **12**, 2967.
52 M. C. Das, S. K. Ghosh and P. K. Bharadwaj, *CrystEngComm*, 2010, **12**, 413.
53 C. A. Ilioudis, D. A. Tocher and J. W. Steed, *J. Am. Chem. Soc.*, 2004, **126**, 12395.
54 D. L. Miller and C. C. Lu, *Dalton Trans.*, 2012, **41**, 7464.
55 S. Saha, B. Akhuli, S. Chakraborty and P. Ghosh, *J. Org. Chem.*, 2013, **78**, 8759.
56 M. Fu and G. Feng, *Chem. Commun.*, 2012, **48**, 6951.
57 G. L. Guillet, F. T. Sloane, M. F. Dumont, K. A. Abboud and L. J. Murray, *Dalton Trans.*, 2012, **41**, 7866.
58 J. M. Chen, X. M. Zhuang, L. Z. Yang, L. Jiang, X. L. Feng and T. B. Lu, *Inorg. Chem.*, 2008, **47**, 3158.
59 X. M. Zhuang, T. B. Lu and S. Chen, *Inorg. Chim. Acta*, 2005, **358**, 2129.
60 (*a*) P. Mateus, R. Delgado, V. André and M. T. Duarte, *Inorg. Chem.*, 2015, **54**, 229; (*b*) G. Y. Xie, L. Jiang and T. B. Lu, *Dalton Trans.*, 2013, **42**, 14092.
61 P. Mateus, R. Delgado, P. Brandão and V. Félix, *Chem. – Eur. J.*, 2011, **17**, 7020.
62 T. Mitra, K. E. Jelfs, M. Schmidtmann, A. Ahmed, S. Y. Chong, D. J. Adams and A. I. Cooper, *Nat. Chem.*, 2013, **5**, 276.
63 T. Hasell, M. Miklitz, A. Stephenson, M. A. Little, S. Y. Chong, R. Clowes, L. Chen, D. Holden, G. A. Tribello, K. E. Jelfs and A. I. Cooper, *J. Am. Chem. Soc.*, 2016, **138**, 1653.
64 L. Chen, P. S. Reiss, S. Y. Chong, D. Holden, K. E. Jelfs, T. Hasell, M. A. Little, A. Kewley, M. E. Briggs, A. Stephenson, K. M. Thomas, J. A. Armstrong, J. Bell, J. Busto, R. Noel, J. Liu, D. M. Strachan, P. K. Thallapally and A. I. Cooper, *Nat. Mater.*, 2014, **13**, 954.
65 Q. Q. Wang, V. W. Day and K. Bowman-James, *J. Am. Chem. Soc.*, 2013, **135**, 392.
66 N. Lopez, D. J. Graham, R. McGuire Jr., G. E. Alliger, Y. Shao-Horn, C. C. Cummins and D. G. Nocera, *Science*, 2012, **335**, 450.
67 M. Nava, N. Lopez, P. Müller, G. Wu, D. G. Nocera and C. C. Cummins, *J. Am. Chem. Soc.*, 2015, **137**, 14562.
68 Y. Dussart, C. Harding, P. Dalgaard, C. Mckenzie, R. Kadirvelraj, V. McKee and J. Nelson, *Dalton Trans.*, 2002, 1704.
69 J. M. Chen, W. Wei, X. L. Feng and T. B. Lu, *Chem. – Asian J.*, 2007, **2**, 710.
70 Q. Q. Wang, V. W. Day and K. Bowman-James, *Org. Lett.*, 2014, **16**, 3982.
71 T. B. Lu, X. M. Zhuang, Y. W. Li and S. Chen, *J. Am. Chem. Soc.*, 2004, **126**, 4760.
72 L. Z. Yang, Y. Li, X. M. Zhuang, L. Jiang, J. M. Chen, R. L. Luck and T. B. Lu, *Chem. – Eur. J.*, 2009, **15**, 12399.
73 H. G. Hao, X. D. Zheng and T. B. Lu, *Angew. Chem., Int. Ed.*, 2010, **49**, 8148.
74 S. M. Barnett, K. I. Goldberg and J. M. Mayer, *Nat. Chem.*, 2012, **4**, 498.